2023

The Effect of Different Fracturing Fluids on the Productivity of Multi-Staged Fractured Marcellus Shale Horizontal Wells

Vida Gyaubea Matey-Korley
West Virginia University, vgm00003@mix.wvu.edu

The Effect of Different Fracturing Fluids on the Productivity of Multi-Staged Fractured Marcellus Shale Horizontal Wells

Vida Gyaubea Matey-Korley

Thesis submitted to the Benjamin M. Statler College of Engineering
at West Virginia University
in partial fulfillment of the requirements for the degree of

Master of Science
In Petroleum and Natural Gas Engineering

Mohamed El-Sgher, Ph.D., Chair
Kashy Aminian, Ph.D.
Samuel Ameri, Ph.D.

Department Of Petroleum and Natural Gas Engineering

Morgantown, West Virginia
2023

Keywords: Hydraulic fracturing, Fracturing Fluids, In Situ Stress, Proppant Transport, Stress Shadow, Fracture Model

ABSTRACT

The Effect of Different Fracturing Fluids on the Productivity of Multi-Staged Fractured Marcellus Shale Horizontal Wells

Vida Gyaubea Matey-Korley

While hydraulic fracturing has undeniably improved the production from oil and gas reservoirs, this technology is not without limitations. The primary hurdles lie in the areas of proppant transport, fluid rheology, and stress management. Despite the extensive research conducted in this domain, there remains a considerable amount of work to be done for comprehensive solutions that account for the complex interactions among fracturing fluid, proppant distribution, and geomechanical conditions. Achieving this will then make room for a holistic and efficient hydraulic fracturing strategy.

This study addresses the above-mentioned problem by examining the impact of fluid type on proppant transport and distribution leading to productivity improvement for a multi-staged fractured Marcellus Shale horizontal well. In addition, stress shadow impact and the extent to which various fracture properties contribute to production are evaluated. The findings can be used to enhance fracture treatment design in the Marcellus shale through optimum fluid selection and stage spacing to reduce the impact of the stress shadow.

Available core plug measurements, well logs, and image logs were analyzed to determine the shale petrophysical and geomechanical properties, including natural fracture (fissure) distribution, to develop a horizontal Marcellus Shale well model. Available laboratory measurements and published data were analyzed to determine the gas adsorption characteristics and the shale compressibility. The impact of the shale compressibility as a function of net stress was then incorporated into the model by developing multipliers for fissure and matrix permeability as well as the hydraulic fracture conductivity. The hydraulic fracture properties estimated using the GOHFER 3D software were incorporated into the developed reservoir model and ultimately, the impact of fluid type and stress shadow on proppant transport and the gas production were investigated.

The reservoir model's credibility was confirmed by a close match between the actual and predicted production. The fracture heights induced by all the fluids remained within the pay zone and the entire fracture height contributed to the production. High Viscosity Friction Reducer (HVFR) resulted in relatively larger fracture volume (with increased fracture height) in comparison to Slickwater, Crosslinked Gel, and Hybrid fluids thus resulting in improved productivity. The cross-linked gel also improved productivity but was found to be inferior to HVFR. High Percentage Reduction indicated the adverse impact of stress shadow on hydraulic fracture properties and gas production. The impact of the stress shadow on the production is, however, more pronounced during early production due to higher production rates.

DEDICATION

This Thesis is Dedicated To

My Family and Friends.

ACKNOWLEDGEMENT

In the pursuit of knowledge and the completion of this thesis, I am profoundly grateful to the Almighty God, whose unwavering presence has been my constancy. I acknowledge His provision of strength and resources to navigate this academic journey.

I would like to express my deepest appreciation to Prof. Ameri Samuel and Dr. Kashy Aminian. The opportunity you both meted out to me, your guidance, expertise and invaluable support have been instrumental in the successful completion of this thesis. Words fall short in conveying the depth of my gratitude to both of you.

A special acknowledgment is reserved for my research advisor, Dr. Mohamed El Sgher. Your support, time, and wealth of knowledge have been pivotal in shaping the outcome of this research. I am truly grateful for your mentorship.

To my respected professors and mentors, I extend my sincere thanks for your mentorship, great teachings and guidance. Your wisdom has been a guiding light, and I am appreciative of the impact you have had on my intellectual growth.

Lastly, but certainly not least, I owe a debt of gratitude to my family, friends, and loved ones. Your support, whether direct or indirect, has been my pillar of strength. Thank you for standing by me and encouraging me throughout this challenging yet rewarding journey.

To you reading this, I acknowledge the light in you and the greater possibility that this light holds in our world. Hope you enjoy this study!

Contents

List of Figures

List of Tables

CHAPTER 1: INTRODUCTION

The United States has emerged as a global leader in crude oil and natural gas production, with tight shale gas and oil formations contributing significantly. These plays are referred to as tight because of their characteristic low permeability. The substantial growth of tight oil and shale gas production is primarily attributed to hydraulic fracturing technology. Matrix stimulation designs, optimization conditions for re-fracturing, and effective reservoir stimulation techniques have garnered significant attention, reflecting hydraulic fracturing's status as a key reservoir-stimulation method.

Hydraulic fracturing, a groundbreaking technique pioneered in 1947, has revolutionized oil and gas extraction. This field has witnessed oil-based fluids, water-based fluids and even gas-based fluids. In fact, the first fracturing job performed in Hugoton field, Kansas in 1947 employed gasoline-based napalm as the fracturing fluid. Environmental and safety concerns led to the usage of water-based fluids, which though relatively better in that regard, has some constraints when dealing with clay-bearing water-sensitive formations. In such situations, liquified natural gas and nitrogen foam are posed as alternatives to water-based fracturing fluids.

Fracturing fluids are mainly used to initiate and propagate fractures and convey proppants into these fractures. Proppants are essential to this process because they form thin layers between fracture faces to prop open the fractures at the latter stage. Linear gels and crosslinked gels/guar have been the traditional fluids used in the industry. These fluids are known for their high polymer activities, thus their high viscosities. With their wall-building characteristics, they can form a layer of filter cake on the fracture faces under pressure, thereby preventing further leak-off of the fluid in the nearby formation. The final stage in the hydraulic fracturing process involves a flowback period where a large amount of the injected fluid can be recovered. These polymer-based fluids are therefore subjected to chemical breakers (mostly enzymes or oxidizers) whose sole purpose is to degrade the polymers for easy recovery and more significantly, for making fractures highly conductive. Unfortunately, the performance of chemical breakers have not been as effective as needed leading to fracture conductivity damage by viscous fluids in very tight formations. Consequently, the “slickwater” with relatively low linear polymer concentration has been developed. The key advantage of slickwater is the reduction in friction loss along flow lines. It,

however, has some constraints with its poor ability to carry proppants due to its low viscosity and the high demand for larger amount of water. This has led to the development of other alternatives like viscoelastic surfactants and energized fluids.

Despite the effectiveness of hydraulic fracturing, challenges persist, particularly in the optimization of fracturing fluid properties and the effective transport of proppants within fractures. As the energy industry continues to evolve, addressing these challenges becomes imperative to ensure sustainable and efficient well stimulation operations.

One other technology mostly used in conjunction with hydraulic fracturing is horizontal drilling. It involves drilling wells along the minimum horizontal principal stress direction. These wells are hydraulically fractured in several stages for production optimization. Production optimization aims to recover the most oil and/or gas possible from a field while maximizing returns (Koray et al, 2023). However, the complex interplay of the stress induced by multiple hydraulic fracture stages and the subsequent stress shadow they generate in the unstimulated reservoir area require comprehensive understanding to optimize fracturing strategies. Understanding how multiple hydraulic fractures propagate with certain fluids and proppants, interact with each other and with natural fractures, and ways to manage stress shadows is therefore critical for effective stimulation designs.

1.1. Problem Statement

In unconventional reservoirs, fluids of low viscosity are often used for hydraulic fracturing treatment. Slickwater fracturing fluid, characterized by its low viscosity, is the predominant choice for hydraulic fracturing in unconventional wells and shale gas reservoirs. Unconventional formations, such as Marcellus Shales, have an abundance of clay minerals in their matrices, which are aligned by gravity during the deposition. This alignment of clay and other minerals creates fine-scale layering. As a consequence, the shale is anisotropic.

The combination of a low viscosity slickwater and stress anisotropy, the latter creating stress barriers between the lower and upper Marcellus, will prevent hydraulic fractures from propagating to all pay zones as the proppant will drop out and concentrate at the bottom. Therefore, this study aims to use different fracturing fluids with high viscosities. By employing fluids with high viscosity, lateral movement occurs at a slower rate, generating pressure buildup that can overcome stress barriers. This, in turn, increases fracture height in the upper Marcellus shale, and ensure a

uniform distribution of proppant throughout the fractures. This topic has not been previously studied.

Another factor influencing fracture propagation is stress shadowing, which subsequently affects proppant transport and distribution. The creation of a hydraulic fracture alters in-situ stresses in the formation, leading to changes in subsequent hydraulic fractures' properties—an occurrence resulting from "stress shadowing." This study, therefore, aims to investigate the impact of two different high-viscosity fluids, two hybrid fluids, and stress shadow on proppant transport and the productivity of a multi-stage fractured Marcellus Shale horizontal well.

CHAPTER 2: LITERATURE REVIEW

2.1. Hydraulic Fracturing

This refers to the artificial creation of fractures in porous media through the pumping of specially designed fluid at a pressure exceeding the formation fracture pressure. Its main purpose is to increase the contact area between reservoir and wellbore for enhanced production of hydrocarbons. The success of a fracturing job is determined by fracture orientation, fracture system extent and the post-treatment production enhancement. The geometry, orientation and extent of the fractures are in turn highly dependent on the in-situ stress state and inherent mechanical properties of the rock. The primary mechanical properties of rock include: strength properties that include compressive and tensile strength, and fracture toughness; elastic properties that involve Poisson's ratio, Young's and Shear modulus; friction; ductility and poroelastic properties. Figure 2.1 below gives an illustration of hydraulic fracturing process while figure 2.2 closely depicts the fracture network system.

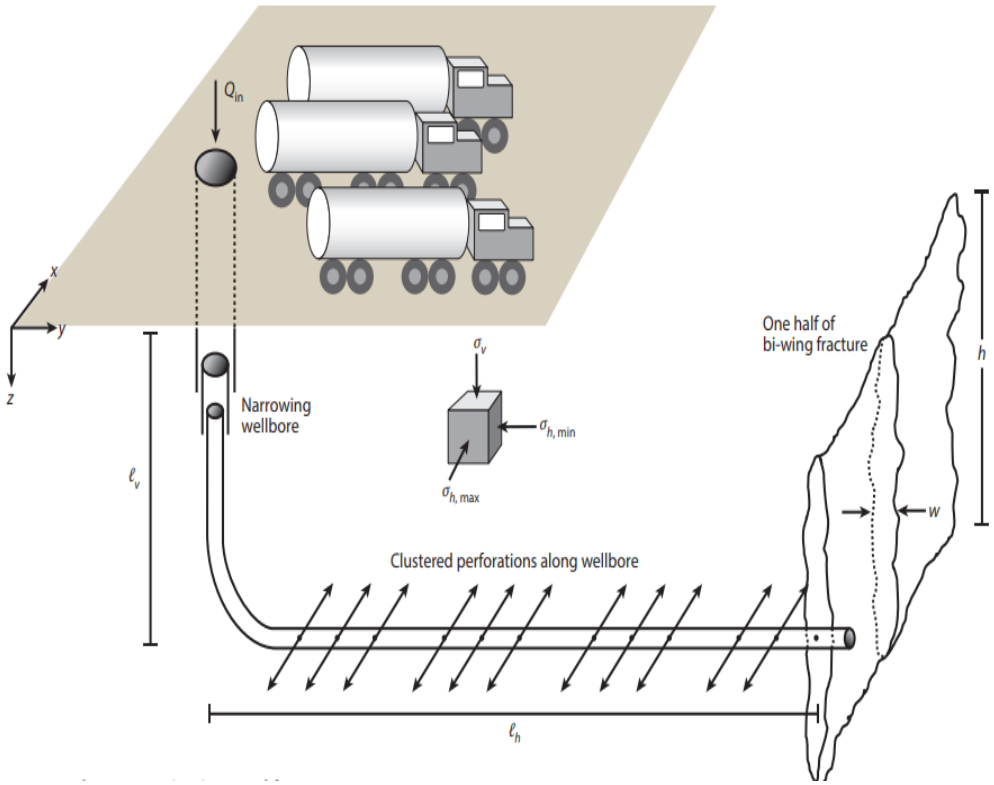

Figure 2.1. The phenomena of transport in fractures and pipes

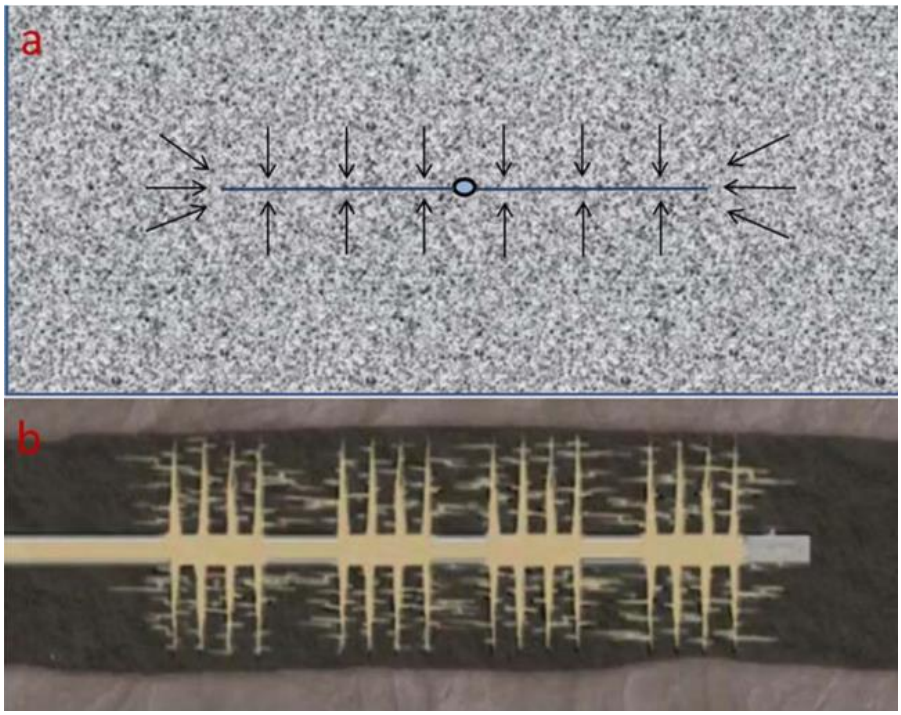

Figure 2.2. (a) Hydraulic fracture in a conventional vertical well (viewed from above), and (b) fracture networks resulting from a multi-staged hydraulically fractured horizontal well in a tight shale formation. (Barati et al. 2014)

2.2. Fracture Orientation and In-Situ Stress State

The transmission of stress among formations is determined by factors such as the tectonic regime in the region, depth, pore pressure, and rock properties. Stress, in its comprehensive form, is represented by a nine-component tensor with six independent values. It is often resolved into normal stress components, those that act perpendicular to a surface, and shear stress components, those that act parallel to a surface. While stress can be defined in any arbitrary orientation, one orientation allows shear stresses to be zero, resulting in stress being defined solely by the three principal stress magnitudes (S3, S2, and S1) along with their orientation. These are generally

known as the minimum horizontal stress (Shmin), the maximum horizontal stress (SHmax), and the vertical stress (Sv) respectively. In a normal faulting environment, the order is Sv > SHmax > Shmin.

The Shmin was traditionally determined by the "mini-frac" technique through an evaluation of induced hydraulic fractures. This was however time demanding and usually costly. The advent of array sonic tools marked a new era in independently assessing compressional and shear wave velocities. Through the utilization of these velocities, coupled with elastic theory, dynamic values of Young's modulus and Poisson's ratio could be extrapolated from sonic log data. Eaton's equation (equation 1, below), based on log-derived Poisson's ratio and assuming elastic behavior with fixed boundary conditions, provides an estimation of Shmin solely from log data. Equation 1:

$$\sigma_{hmin} = \left(\frac{v}{1-v}\right)(\sigma_v - \alpha Pp) + \alpha Pp \qquad (1)$$

Where: σ_{hmin} is minimum horizontal stress, σ_v is vertical stress estimated from rock density, v is Poisson's ratio (from the fracture log), Pp is formation pore pressure, and α is Biot's coefficient; usually assumed to be 1.0.

The known fact that fractures propagate along a path of least resistance highlights the influence of variations in in-situ stresses on fracture propagation in reservoir formations. The in-situ stress field ultimately determines the size and orientation of a fracture, as well as the pressure magnitude needed for its creation. To be more effective, hydraulic fractures must be oriented in alignment with the reservoir's flow properties. Natural reservoirs have anisotropic permeability, meaning that their permeability varies in different directions. Permeability is generally lowest through the bedding plane. Therefore, it is best to create fractures with path flow perpendicular to the bedding plane. Under the influence of in-situ stress state, fractures tend to propagate perpendicular to and open in the direction of the minimum compressive stress. This is because the minimum compressive stress is the weakest direction in the rock, and therefore the easiest direction for fractures to propagate.

2.3. Natural Fractures and Hydraulic Fractures

Fractures in rocks arise from natural stresses and fluid movement, contributing significantly to shale gas reservoirs. Efficient drilling and hydraulic fracturing processes aim to intersect the natural fracture network. Natural fractures can be described by their orientation, length, aperture, and roughness. The natural fracture network may exist in percolated or unpercolated states, displaying both heterogeneous and anisotropic qualities.

Preexisting fractures, faults and joints have the potential to alter the propagation direction of induced fractures. In conventional reservoirs, lithostatic stresses generally dictate the global fracture orientation, with preexisting features having limited impact. However, in unconventional reservoirs, especially fractured source rocks, the interaction between hydraulic fractures, bedding planes, and preexisting fractures becomes crucial, influencing the stimulated reservoir area. The extent to which a hydraulic fracture interacts with preexisting features depends not only on the geomechanical setting but also on the fracturing fluid, introducing another layer of complexity to fluid selection in fracturing operations.

2.4. Pressure terms associated with Hydraulic Fracturing

Understanding the various pressure terms associated with fracking is crucial for optimizing the fracturing process and ensuring well integrity. This section therefore introduces the key pressure terms associated with hydraulic fracturing.

2.4.1. Near-wellbore friction pressure

Friction pressure near the wellbore, generally termed Near-Wellbore Friction Pressure (NWBFP), encompasses the overall pressure drop near the wellbore. NWBFP represents the sum of tortuosity and perforation friction pressure.

2.4.2. Closure pressure

Closure pressure, the least amount of pressure required to maintain open fractures, is defined as the pressure at which a fracture closes in the absence of proppant. Below this threshold, the fracture remains closed, while above it, the fracture stays open. Challenges in initiating frac job stages may arise from not surpassing closure stress, especially in zones with high closure stress. Consequently, it is strongly recommended to position the wellbore in a zone with higher closure pressure both above and below to contain fractures. Closure pressure is often assumed to be equivalent to the minimum horizontal stress. The determination of closure pressure can be achieved through a DFIT

or a step-rate test. The step-rate test, conducted prior to the frac job, helps determine the fracture extension pressure (PEXT), which is typically slightly higher than the fracture closure pressure. The test therefore serves to establish the upper limit of closure pressure and is thus instrumental in hydraulic fracturing design.

2.4.3. Fracture extension pressure

Fracture extension pressure, which is synonymous to bottom hole treating pressure (BHTP), denotes the pressure within the fracture(s) responsible for their growth during continuous pumping. Essentially, it is the pressure within the frac fluid in the fracture necessary for propagating the fracture. To sustain open fractures and facilitate their expansion, the fracture extension pressure must surpass the closure pressure of the formation. This is crucial as the extension pressure represents the energy needed to actively drive the fracture propagation, rather than merely maintaining its openness. In hard formations, the fracture extension pressure closely aligns with the closure pressure. Conversely, in softer formations, where plastic deformation at the fracture tip absorbs substantial energy, the extension pressure can significantly exceed the closure pressure.

2.4.4. Net pressure

Net pressure, also known as process zone stress, signifies the energy essential for propelling fracture growth and expanding width. It represents the surplus pressure beyond the fracturing fluid pressure necessary for extending fractures and is basically the difference between pressure of the fracturing fluid and closure pressure. The greater the pressure within a fracture, the higher the potential for growth. It is worth noting that the term "net pressure" is applicable only when the fracture is open; if the fracture is closed, the net pressure amounts to null. Various factors, including fracture height, fluid viscosity, fluid rate, Young's modulus, total fracture length, and tip pressure, influence net pressure. Equation 12 below is used for the calculation of net pressure.

$$P_{net} = P_{bh} - \Delta P_{nwb} - P_c \tag{12}$$

Where: P_{bh} is the bottomhole treating pressure in psi, P_{nwb} is the near wellbore pressure in psi, P_c is the closure pressure in psi and P_{net} is the net pressure in psi.

2.4.5. Wellhead (Surface) treating pressure (STP)

In simple terms, it refers to the pressure at the surface during frac treatment. It denotes the real-time pressure recorded from the surface pressure transducer on the main line. Accurate estimation of surface-treating pressure is crucial to ensure an adequate hydraulic horsepower (HHP) is available on-site for the frac job. The HHP required is a function of both the surface-treating rate and surface-treating pressure. STP is determined by the equation 13 below:

$$STP = P_{bh} + P_f - P_h + P_{net} \quad (13)$$

Where: P_{bh} is the bottomhole treating pressure in psi, P_f is the total friction pressure in psi, P_h is the hydrostatic pressure in psi and P_{net} is the net pressure in psi.

2.4.6. Maximum Treatment Pressure

The peak treatment pressure is anticipated during the breakdown of the formation. At this point, the bottom-hole pressure equals the formation breakdown pressure, and the surface pressure can be determined using the following equation (14):

$$P_{si} = P_{bd} - \Delta P_h + \Delta P_f \quad (14)$$

Where:

P_{bd} is breakdown pressure (psi), ΔP_h is hydrostatic pressure drop (psi), ΔP_f is frictional pressure drop (psi) and P_{si} is surface injection pressure (psi).

2.5. Fracturing Fluids

The success of fracturing treatment is attributed to the development of advanced fracturing fluids and optimal proppants that play pivotal roles in enhancing reservoir permeability and hydrocarbon recovery. Some key factors to consider in fluid selection include viscosity, which determines the transport/suspension of proppant, fracture width, and fluid-loss control; and cleanliness (post-flowback) to achieve optimal post-fracture conductivity. The evolution of fracturing fluids began with the linear guar gels (and its derivatives), to crosslinked gels, and the subsequent development of slickwater (waterfracs), viscoelastic surfactants (VES), energized fluids and guar alternatives.

2.5.1. Linear Gel

The simplest and earliest fluid category employed in fracturing treatment is linear gel. The first kind utilized was water with starch as a viscosifier until guar gum emerged as a replacement in the early 1960s. This shift was primarily due to issues with starch's temperature instability, susceptibility to shear, and vulnerability to bacterial degradation. Guar is regarded as the most economical polymer and it is known to leave substantial amount of insoluble residue behind. It is a leguminous crop predominantly cultivated in India and Pakistan, often harvested manually as a secondary crop by subsistence farmers. Guar serves multiple purposes, being utilized for both human and cattle food, with its seeds capable of being ground into powder. This is seen in figure 2.3. While it is commonly employed as a slurry concentrate, Guar can also be utilized as a dry powder that is mixed on “fly”.

Guar, as a high-molecular-weight polymer consist of galactose and mannose sugars in a long-chain structure, and is commonly employed to thicken water for fracturing. Its concentration for this purpose generally ranges from 0.12% to 0.96% w/w. The polymannose (complex sugar) backbone of guar is insoluble, though the galactose branches impart water solubility. This explains a 6-10% by weight insoluble residue from guar. Aside from this residue, the chemical breakers (especially enzymes) yield extra residues. Guar derivatives are also commonly used, and these are made by subjecting guar powder to elevated pH water and high temperature in reaction with derivatizing agents like propylene oxide (which produces hydroxypropyl guar -HPG). The normal mixture of the guar or its derivatives with water and additives for fracturing gives rise to the linear gel. Other Guar derivatives include carboxymethylhydroxypropyl guar (CMHPG), which is double-derivatized; and carboxymethylhydroxyethylcellulose (CMHEC) which is a cellulose derivative.

Due to the cheaper price of guar, linear gels serve as a cost-effective fracturing fluid. However, they are demerited with their limited shear recovery, viscosity degradation with time, temperature sensitivity, and susceptibility to breakage.

Figure 2. 3. The Guar plant (left) and powder (right) (Source: Altrafine gums)

2.5.2. Crosslinked Fluids

For deep penetration of proppant or acid away from the wellbore, linear gels couldn't live up to the task. Though there is some simplicity when it comes to their use and control, their relatively less temperature stability and poor proppant suspension make them quite unfavorable. Crosslinked fracturing fluid addresses such problems through their lack of sensitivity to shear (El Sgher et al, 2023) and better temperature stability. They are formed when the various molecules of a base polymer are tied into a structure through metal, metal chelate or borate crosslinkers. In essence, cross-linkers elevate molecular weight without the need for extra polymers. From an economic standpoint, generating a high-viscosity fluid with a linear gel is significantly more costly than employing a cross-linked fluid system. For instance, the expense incurred in utilizing a linear gel to produce a fluid system with a viscosity of 180 centipoise is considerably higher than using a cross-linked fluid system to achieve the same viscosity. With their cost-effectiveness, lack of shear sensitivity and the development of many breakers for controllable degradation, the guar/borate fluids serve as a dominant crosslinked system employed. Guars are also crosslinked with ions of elements like zirconium, titanium, and aluminum.

Borate ions serve as the predominant crosslinking agents in guar polymer applications. Borax (sodium tetraborate decahydrate) and boric acid (along with caustic soda) are commonly employed

as sources of borate ions for crosslinking guar, with crosslinking agent concentrations ranging from 0.024 to 0.09% w/w. Additionally, Colemanite and ulexite, primarily composed of low-solubility calcium or calcium- or sodium-borate, find application in high-temperature scenarios or when a delayed crosslink is necessary to minimize friction pressure before reaching the formation. Organo-borates also present an alternative for crosslinking guar chains.

Regardless of the kind of boron introduced into the fluid, the crosslinking species which is primarily monoborate, engages in hydrogen bonding (or potentially ionic bonding) with the cis-hydroxyls on the guar. This interaction results in the formation of inter- or intra-molecular crosslinking, or a combination of both. The presence of monoborate and polyborate ions is contingent upon temperature pH, and ionic strength.

pH suitability of crosslinkers

Titanate and zirconate exhibit effectiveness across a broad pH range 3 to 11, whiles borate ions demonstrate efficacy only between pH 8 and 11. Aluminum's effectiveness is confined to the pH range of 3 to 5.

Temperature suitability of crosslinkers

Zirconate can be employed at temperatures as high as 400°F, while titanate and borate are effective at temperatures up to 325°F. Aluminum, however, can only be utilized at temperatures below 150°F.

Depending on the temperature, borate can be used at pH values of 7.5 and above. Despite borate crosslinks showing less susceptibility to shear rate and shear history compared to other metal ions, some sensitivity to shear history, particularly during initial-time viscosity development, has been reported (Barati et al, 2014).

Guar-borate gels exhibit remarkable resistance to permanent degradation under shear. The process of breaking and reforming borate-polymer complexes under shear is continuous. These gels quickly reheal after breakdown because the time required for recrosslinking through interchain contacts is less than 1 ms. This rapid recovery is attributed to the swift exchange equilibrium of borate acid and monoborate ion. With an increase in temperature, it becomes necessary to elevate the pH to compensate for the reduction in borate ion concentration and the resulting exponential decrease in interchain contacts. Moreover, as temperature rises, a higher polymer concentration is

essential to maintain sufficient interchain contacts, ensuring an ample number of crosslinks for achieving the desired high final viscosity in the fracturing fluid.

Fluids crosslinked with titanium and zirconium have demonstrated reduced fracture conductivity and increased face damage when compared to fluids crosslinked with borate. The former are primarily utilized in reservoirs with exceptionally high temperatures, where borate-crosslinked fluids are not effective. Also, generally, crosslinked fluids are more applicable to shale oil applications when higher fracture conductivity is required, and the converse is better applied with the use of slickwater and hybrid fluids (Barati et al, 2014).

2.5.2.1. Delayed Crosslinked gels

This entails a crosslinked fluid system in which the duration for crosslinking is regulated. The rate of crosslinking can be managed through various factors like fluid temperature, the type of crosslinker, shear conditions, and the presence of organic compounds that react with the crosslinker. The delayed cross-linking process slows down the cross-linking of the fluid, reducing friction within the pipe as the fluid traverses extensive lengths. Once the fluid pass through the pipe, the cross-linked fluid resumes its normal functionality, endeavoring to navigate the tortuous path post-perforations and prior to reaching the main body of fractures.

A delayed crosslinked system offers several key benefits, including improved dispersion of the crosslinker, enhanced long-term stability at elevated temperatures, reduced friction pressures enabling higher injection rates, and decreased horsepower requirements.

In totality, Crosslinked gels have gained prominence due to their enhanced stability and efficiency in hydraulic fracturing operations. These gels offer superior viscosity and fracture-carrying capacity, contributing to improved well performance. To ensure controlled degradation post-fracturing, breakers are commonly employed to facilitate the breakage of crosslinking bonds, allowing for easier fluid recovery and reduced formation damage. However, it is crucial to acknowledge that despite the advantages of crosslinked gels and the incorporation of breakers, a persistent challenge exists in the form of residual material. These residues, though diminished by breaker action, can still be present in the fracturing fluid post-operation as shown in figure 2.4.

The potential impact of these remnants on well productivity, formation permeability, and overall reservoir performance necessitates careful consideration.

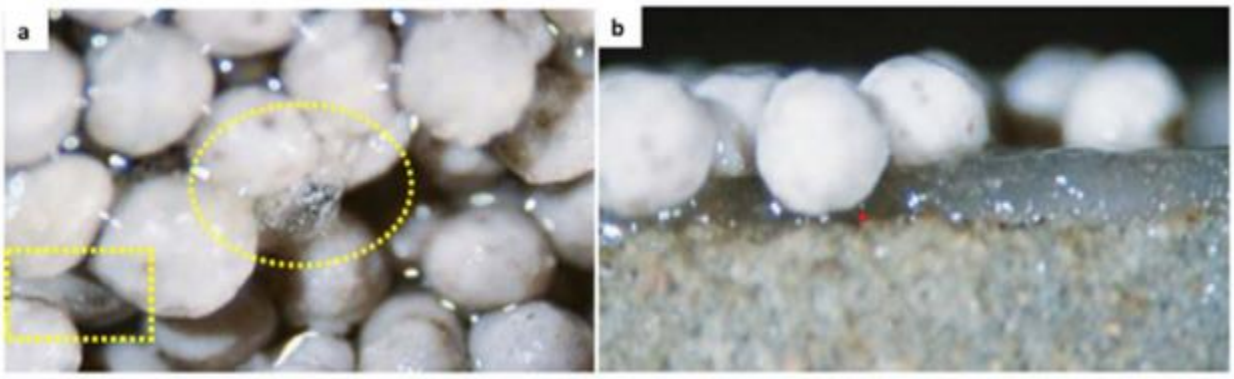

Figure 2.4 (a) Residual gel damage persisting after breaking a Zirconate XL CMHPG (at 35 ppt) in a long-term conductivity cell. (b) illustrates a filter cake build-up of the XL gel in (a) (Barati et al. 2014)

2.5.3. Slickwater

Slickwater treatments employ high volumes of water with added polyacrylamide or minimal linear gel as a friction reducer, resulting in issues such as poor proppant transport and narrow fracture widths. To mitigate these problems, higher injection rates and lower proppant concentrations have been used. Slickwater treatments offer advantages like reduced cost, reduced fracture height growth and lower gel damage, but they are associated with challenges like poor proppant transport, narrower fracture widths, higher leakoff and complex fracture geometry, leading to reduced fracture conductivity compared to crosslinked fluids (El-Sgher et al. 2023).

In relation to the complexities that can occur from the use of slickwater, it is worth noting that in reservoirs where pre-existing cross-cutting fracture systems and relatively uniform horizontal stresses are prevalent, the creation of a complex fracture network is a sought-after objective. Interestingly, even though this complexity may result in the formation of lower conductivity fractures, the advantages they bring often outweigh the drawbacks. This complexity translates into increased reservoir contact, a highly desirable outcome, especially in shale gas reservoirs where

hydrocarbons struggle to traverse the rock on their own. To be more specific, when compared to crosslinked fluids, slickwater treatments tend to create more symmetric microseismic event clouds. This is because the viscosity of the fracturing fluid is inversely proportional to both the equation for the flow of fluid in natural fractures and the equation for pressure diffusion in the rock fabric. Below is the "cubic equation" for flow in parallel plates. Equation 2:

$$Q = \frac{\gamma_w}{\mu} G a^3 \Delta h \quad (2)$$

Where Q is flow rate, γ_w is fluid density, Δh is pressure drop, μ is fluid viscosity, G is geometry constant, and a is fracture aperture. From the equations, a decrease in frac fluid viscosity results in a greater penetration of fluid pressure into the rock fabric, creating a more symmetric microseismic event cloud. Consequently, although slickwater may hinder proppant transport, it proves advantageous in expanding the potential area influenced by shear stimulation. However, it's important to note that high pump rates are not conducive to shear stimulation. The diffusion of pressure into the rock fabric is inversely related to viscosity and directly linked to time, specifically the time of applying the driving pressure for diffusion. Consequently, when pump rates are higher, and the fluid volume is fixed, there is a reduction in the overall time available for pressure diffusion to take place. The significance of pressure diffusion in generating shear stimulation is evident in the nearly universal observation of microseismic events occurring after injection pumps have been shut down, but pressure diffusion continues through the rock fabric (Nagel B.). Thus, to maximize slickwater treatments, high pump rates should be avoided.

2.5.4. Viscoelastic Fluids

Researchers addressed the issue of proppant pack damage caused by residual fractions from incompletely broken fracturing fluids by developing viscoelastic surfactant (VES)-based fluids. These fluids are shear-thickening but leave minimal residues. They consist of hydrophilic and hydrophobic groups that self-associate to safeguard their nonpolar segments and prevent them from contacting the water-phase. In aqueous solutions, they form micelles to boost viscosity

without the need for crosslinking agents. The structure swells, breaking into smaller micelles when exposed to organic fluids, causing viscosity reduction and eliminating the need for additional breakers. However, VES-based systems pose challenges like cost concerns, high fluid leakoff due to inadequate wall-building, and unwanted viscosity reduction at elevated temperatures.

2.5.5. Energized Fluids

The energized fluid systems feature substantial gas fractions and minimal water content. These systems offer notable benefits, including damage reduction from capillary pressure, relative permeability inconsistencies, and fluid invasion. Additionally, their multiphase nature reduces fluid loss volume, potentially leading to decreased water usage or expanded fracture networks for a given water volume. There is also the added effect of minimal water contact with water-sensitive clays, and the enhanced hydraulic conductivity recovery due to the free gas and dissolved gas occupying the near fracture area. Typical examples of these fluid systems include CO2 and nitrogen foams using crosslinked guar solutions, nitrogen foam generated by a foaming agent and HPG solutions, CO2 and nitrogen foaming of the VES gels, and Polyemulsions which are hydrocarbons that are emulsified as an external phase with water, e.g., diesel (Barati et al. 2014).

2.5.6. Friction Reducers (And High Viscosity Friction Reducers)

The need for guar alternatives became imperative at the global shortage of guar and the industry's demand for friction reducers capable of transporting proppants. Synthetic associative acrylamide-based polymers formed by a modification with monomers like sodium acrylate have auspicious prospects. Associative polymers demonstrate higher viscosity at lower shear rates, rendering them advantageous for facilitating proppant transport within fractures. These polyacrylamides (PAM) tend to be highly water-absorbent and demonstrate great temperature stability with the added ability to withstand high salinity environments. The main demerit of the usage of this fracturing fluid is their relatively high cost. Firstly, friction reducers are employed to reduce pumping resistance along lengthy lateral sections, influencing job expenses by reducing friction and subsequently lowering the required hydraulic horsepower. Secondly, in higher quantities, they

transform into high-viscosity friction reducers (HVFR), wherein they act as viscosifiers, offering an additional advantage of being capable of accommodating higher proppant concentrations. HVFR fluids are superior for suspending smaller-sized sand proppants, even when compared to low viscosity fluids like slickwater and freshwater. However, under low loading of HLFR, these fluids prove ineffective as transport systems for larger particles with relatively high densities, such as 20/40 mesh sand (Faraj et al, 2019).

The polyacrylamide-based friction reducers are typically manufactured as water-in-oil emulsions. This emulsion type has increased stability due to the immiscibility between oil and water. The oil phase helps protect the friction reducer polymer from degrading and to also prevent it from gelling. Friction reducers are added "on the fly" to the fracturing fluid and effectively minimize energy loss through the conversion of turbulent flow into laminar flow via their turbulent eddies interactions. Consequently, reduction of flow friction within macro tubing is achieved. These oil-in-water emulsion particles are generally quite small and can smoothly block the microfractures, micropores and matrix of gas shale formations (Sun et al 2013).

Sun et al. (2013) explored the flow characteristics of friction reducer solution within microfractures using a micro-sized fracture model in their study. A commercial friction reducer was formulated with deionized water at a notably low concentration. Initially, the size of the emulsion particles in the friction reducer solution was examined across both micrometer and nanometer scales. Subsequently, the friction reducer solution was introduced into the microfractures at various velocities. It was observed that the pressure gradient increased with increasing concentration of FR and decreased with increasing velocity. The apparent viscosity of the FR solution was relatively higher than water. In addition, the FR solution did not reduce the flowing friction in the microfracture. Also, the shear rate, which is a measure of the velocity gradient of the fluid, influenced the apparent viscosity of the fluid. At higher rates, fluid's apparent viscosity was seen to decrease. This indicates the shear thinning characteristics of friction reducer solutions and is further corroborated by Faraj et al (2019). It was also found that the apparent viscosity of FR solution is higher at lower shear rates and could be explained by the boundary layer theory. The boundary layer is a thin layer of fluid near the surface of a solid boundary where the fluid velocity is reduced due to viscous drag. Its thickness increases with distance from the surface. In macro tubing, the injection pressure of the FR solution was significantly lower than that of water, whereas in a microfracture, the injection pressure of the FR solution exceeded that

of water. This is due to the inability of the FR solution to attain turbulent flow within the microfracture, leading to heightened flowing friction. In comparison with water, the FR solution faces challenges in penetrating microfractures, potentially resulting in reduced contamination in gas shale microfractures during slickwater stimulation. Additionally, at same velocities, the FR solution exhibits greater residual resistance in larger microfractures compared to smaller ones.

2.5.7. Hybrid Fluids

A notable approach in modern hydraulic fracturing operations is the utilization of a hybrid fluid design. This strategy involves the use of a low-viscosity fluid in the initial stages, particularly in the pad and early proppant stages. As the operation progresses, proppant concentrations are typically increased, and larger mesh proppants are introduced. To accommodate these changes and effectively place larger diameter proppants, a shift is made to a higher viscosity fluid, often supplemented with extra-large proppants.

Also, in unconventional reservoirs, certain companies opt for this type of fracturing method when encountering significant challenges in introducing high proppant concentrations into the formation. This is particularly relevant for formations that are not conducive to higher proppant concentrations. In such cases, the only viable options for effectively placing the designated sand involve using either linear gel, which is less viscous compared to cross-linked gel, or employing cross-linked gel at higher proppant concentrations.

This hybrid fluid approach ensures that the fracturing process is finely tuned to the specific needs of the reservoir, optimizing proppant placement and fracture complexity.

2.6. Fluid Additives

Various additives like friction reducer, scale inhibitor, acid, corrosion inhibitors, biocides, surfactant, potassium chloride, iron control agents, and pH adjusting agents are introduced into different fracturing fluids for specific purposes. Fluid additives used in the industry are listed below:

2.6.1. Friction reducers

These are employed to minimize friction as fluid is pumped down the well tubulars and pipings, thereby reducing drag in them. Friction reducers that are highly efficient and cost-effective in fracturing fluids typically consist of polymers and copolymers of acrylamide at low concentrations.

2.6.2. Fluid Loss additives

When applied, these form filter cake to reduce fluid leak off into the formation. Common materials used for this purpose include guar gum, calcium carbonates, silica flour, natural starch, oil soluble resin, and lignosulfonate.

2.6.3. Buffers

These are primarily used to maintain or regulate the pH of the base fluid, where pH represents the acidity or basicity of the fluid. Two types of buffers are employed in the industry. The first type is known as an acidic buffer, utilized to accelerate the gel hydration process. The second type, termed a basic buffer, is employed in conjunction with cross-linked fluid to induce delayed cross-linking. Typical examples include potassium, soda ash, fumaric acid, ammonium, sodium bicarbonate or a combination of these.

2.6.4. Breakers

Breakers or gel breakers are added to facilitate controlled degradation of a viscous fracturing fluid into a thinner fluid, thus allowing for easy extraction from the fracture. This process aims to boost the permeability of the proppant pack to oil and gas, thereby enhancing the overall effectiveness of the treatment. The extent of gel reduction is governed by factors such as the type of breaker, breaker concentration, temperature, gel concentration, time, and pH. To verify the appropriate reduction in viscosity post-breakage, the gel breaker can be tested at the surface by heating it to the formation temperature using a bath. Typical breakers include oxidizers and enzymes.

2.6.5. Bactericides

These prevent viscosity losses resulting from bacterial degradation of polymer. Typical examples are chlorophenates, glutaraldehyde, quaternary amines and isothiazoline.

2.6.6. Surfactants

These are mainly employed to lower the surface tension of the fracturing fluid for enhanced fluid recovery and compatibility between the fracturing fluid and the formation matrix as well as the formation fluids. There are different types of surfactants used in the industry. Some of these include:

Microemulsions: These surfactants alter the contact angle between liquids and surfaces, enhancing wetting and promoting improved fluid recovery during flowback.

Nonemulsifiers: These deter or reduce the formation of emulsions and are particularly employed in formations containing oil or condensate. Emulsions can impede fluid flow and complicate separation processes.

Foamers: These surfactants produce stable foam, acting as a carrier for proppant transport. Foamers guarantee the uniform distribution of proppant particles across the fracture network.

Typical surfactants used in the industry are isopropanol, methanol and ethoxylated alcohol.

2.6.7. Clay stabilizers

Commonly added to prevent clay disintegration, which has the potential to cause bridging of narrow pores and subsequent permeability reduction. Typical clay stabilizers include potassium chloride, calcium chloride, ammonium chloride and polymeric clay stabilizers.

2.6.8. Iron Controls

These are employed to manage and avoid the presence of dissolved iron in fracturing fluid. They inhibit the precipitation of certain chemicals like sulfates and carbonates, which have the potential to plug pores and openings in the formation. Examples include, citric acid (a food additive), glycol, ammonium chloride, and ethylene.

Fluid compatibility and formation compatibility tend to be the two primary factors to consider when it comes to fluid and chemical selection for hydraulic fracturing. Importantly, the choice of chemicals is contingent on the type of water utilized. Typically, a significant portion of water from the drilled wells is employed, and this water is commonly treated to eliminate solids and bacteria.

Unfortunately, the dissolved solids, mainly salts, are often retained due to the associated expenses of removal and disposal challenges. It has been established for quite some time that fluids with elevated total dissolved solids (TDS) negatively impact the effectiveness of certain friction reducers.

Alotaibi et al (2023) delved into the influence of chemicals on performance rates in Bakken Shale wells. Their study proved that anionic friction reducers, with their negatively charged functional groups, are effective in certain fracturing fluids, especially under subsurface formation conditions. Kitchen et al (2023) focused on optimizing performance using friction-reducer boosters for slickwater and high-viscosity fluids. Anionic friction reducers demonstrated suitability for mid-salinity environments. To improve their performance in highly saline environments, higher polymer activity and specific monomers like sulfonated or cationic were required. However, this must be carefully done as the combination of an anionic friction reducer and a cation (such as iron) can be quite deteriorating. It is known that when these meet, the polymers in the additive tangle and coil on themselves; and friction reducers exhibit optimal performance when the polymers are stretched out in the direction of the flow. In extreme tangling levels, semisolid amalgams of friction reducer polymers can form. These are informally referred to as “gummy bears”. Friction reducers come in liquid or dry form and generally, polymer solutions' properties were governed by monomer composition, molecular weight, and concentration (Xiong et al 2018).

2.7. Proppant Transport and Distribution

At a point in the fluid injection process of hydraulic fracturing, proppants will be introduced to prop open these fractures. The amount of proppant injected is determined by the initial fracture design and the characteristics of the reservoir formation.

The movement of proppant particles occurs in both vertical and horizontal directions. In the horizontal direction, proppant particles move at the same velocity as the fluid, following the fracture tip. In the vertical direction, however, proppant velocity, which is the settling velocity between the fluid and proppant particles. This is as a result of slippage and gravitational forces, causing them to settle at a slower rate than the fluid. A commonly overlooked aspect of proppant movement lies in its progression within the fracture width, often dismissed due to the scale effect where the fracture width is significantly smaller than the fracture length and height. As proppant

particles gradually settle, they occupy the fracture width, thereby amplifying the proppant concentration in the vertical cross-section. Beyond a critical concentration threshold, the occurrence of screening out, also known as sanding off, takes place. The pace at which the proppant bank grows or screening out occurs is contingent upon the settling velocity of the proppant. The settling velocity of an individual, perfectly spherical proppant particle can be determined by applying Stokes' law, assuming an infinitely large fracture and neglecting boundary effects. The settling velocity is then established for various flow regimes based on the dimensionless Reynolds number. It must be noted that dimensionless quantities are of great significance in characterizing the fracture properties and fracturing treatment effectiveness. Notably, the Reynolds number (Re) serves as an indicator of the relative strength of viscous and inertial forces, the Weissenberg number (Wi) provides insights into the elastic nature of the fluid, and the Stokes number (Sk) quantifies the importance of particle inertia in unsteady flows.

Reynold's number is mathematically expressed as in equation 3 below:

$$R_e = \frac{\rho_f w^2 \gamma}{\mu} \tag{3}$$

Where: R_e is the Reynolds number, $\rho_f$is the fluid density, w is the fracture width, γ is the shear rate and μ is the fluid viscosity.

For flow regimes with Reynolds number lower than 2, the settling velocity of proppants is determined by equation 4 below:

$$V_{ps} = \frac{g(\rho_p - \rho_f)d_p^2}{18\mu} \tag{4}$$

Where Reynolds number is in the range of 2 and 500, the settling velocity of proppant particles is defined as in equation 5:

$$V_{ps} = \frac{20.34(\rho_p - \rho_f)^{0.71} d_p^{1.14}}{\rho_f^{0.29} \mu^{0.43}} \tag{5}$$

Where Reynolds number is greater than 500, the settling velocity of proppant particles is quantified by equation 6 below:

$$V_{ps} = 1.74\sqrt{\frac{g(\rho_p - \rho_f)d_p}{p_f}} \quad (6)$$

With V_{ps} being the proppant settling viscosity from Stokes law, $\rho_f \; and \; \rho_p$being the fracturing fluid and proppant density respectively, μ being the dynamic viscosity of the fluid and d_p being the diameter of proppant.

Owing to the limitations via assumptions made in obtaining settling velocity of proppants from the Stokes law (that is, infinitely large fracture assumption and the neglect of proppant particles interaction), a corrected version given by Gadde et al. (2004) is used, and this is shown in equation 7 below:

$$V'_{ps} = V_{ps}\left[\,0.563\left(\frac{d_p}{w}\right)^2 - 1.563\left(\frac{d_p}{w}\right) + 1\right](2.37c^2 - 3.08c + 1) \quad (7)$$

Where V'_{ps} represents the corrected velocity and c denotes the proppant concentration.

Also, the viscosity of the fracturing fluid will change as proppant settles. The relationship between the change in fracturing fluid viscosity and proppant concentration can be determined via the equation 8:

$$\mu = \mu_0 \left\{1 + \left[\,0.75(e^{1.5n} - 1)e^{\frac{-a(1-\eta)}{1000}}\right]\frac{1.25c}{1-1.5c}\right\}^2 \quad (8)$$

Where $a \; and \; \eta$ are the non-Newtonian fluid constants and μ_0 denotes the uncorrected viscosity of the fracturing fluid.

It must be noted that the settling velocity of proppant plays a pivotal role in influencing both proppant distribution and fracture conductivity during hydraulic fracturing. Failure to consider proppant settling may result in an overestimation of well productivity, particularly in tighter formations and when employing larger proppant sizes. Precise modeling of proppant settling is essential for the effective optimization of hydraulic fracturing designs.

In very low permeability formations, there exists a critical proppant size, and employing a combination of small and large proppant sizes can enhance well productivity to its maximum potential.

2.8. Proppants

Proppants are introduced into the fracture to enhance conductivity (prop open fractures) after pressure or flow is halted from the surface. They are classified by their ability to withstand closure stress, the size and distribution of their grains, the amount of fines they contain, their roundness and sphericity, and their density (Barbarti et al., 2019). The accurate selection of proppant types and sizes holds significant importance in hydraulic fracturing treatments, as it directly impacts the size of the fractures that propagate. The type of proppant when used with a consistent proppant size (e.g., 40/70 mesh) and concentration (2.0 lb/ft^2), will exhibit distinct behaviors.

2.8.1. Proppants physical properties

2.8.1.1. Size of proppant grain and grain size distribution

Proppant sizes typically range between 8 and 140 mesh (105 µm - 2.38 mm). They are commonly expressed as sieve cut, with such examples as 70/140 mesh (105 µm - 210 mm), 40/70 mesh (210 µm - 420 mm), 30/50 mesh (297 µm - 595 mm), 20/40 mesh (420 µm - 841 mm), and 16/30 mesh (595 µm - 1190 mm). Mesh size refers to the number of openings across one linear inch of screen. (Feng Li et al, 2016).

It is widely acknowledged that proppant permeability is directly proportional to proppant size. As the mesh size of the proppant increases, both proppant porosity and permeability experience a rise. In the 1980s and 1990s, 20/40 proppant which is a mixture passing through a 20 mesh filter but retained on a 40 mesh pan, was prevalent in most conventional plays and persisted into the early years of unconventionals. Although 100 mesh proppant was available in the industry, it was not commonly utilized as a proppant due to its low conductivity and strength as natural sand. Instead, it found frequent use for leakoff control. The use of 100 mesh proppant became popular in the early 2010s due to its reported successes in unconventional plays such as the Barnett. This was driven by the need to address concerns over proppant transport in low permeability formations, as well as the belief that even the low conductivity of 100 mesh sand would be sufficient. Today, estimates suggest that over 50% of frac sand is 100 mesh or finer.

2.8.1.2. Proppant roundness and sphericity

The roundness of proppant grains gauges the sharpness of their corners or curvature, while particle sphericity assesses how closely the proppant particle or grain approaches a sphere. The ideal shape of proppant is the spherical shape and non-angular. In such a case, stresses are distributed more evenly on the proppants, resulting in a tighter proppant pack. Angular grains are prone to failure at lower closure stresses, leading to fines production and a reduction in permeability.

2.8.1.3. Proppant density

The settling rate of proppants exhibits a linear increase with density. Suspending high-density proppants in fracturing fluids and efficiently transporting them to the top of the fracture pose challenges. To counter settling, high-viscosity fluids are employed or the injection rate is increased to reduce the necessary suspension time.

2.8.1.4. Strength of Proppant

Insufficient proppant strength may result in the crushing of proppants under closure stress, generating fines. The fluctuating closure stress in fractures, caused by well shut-ins, subjects proppants to stress which leads to adjustments in their arrangement within the pack. This occasionally results in proppant embedment, a phenomenon where proppants become buried in the fractured surface, generating smaller particles (fines) and sometimes causing proppant crushing due to closure stress. This embedment significantly affects fracture geometry (typically a reduction in fracture width) and conductivity. The strength of a proppant plays a vital role in its ability to resist embedment due to closure stress. Deeper formations are anticipated to exert higher closure stress. In shallower formations, low-strength proppants can be utilized since the applied stress may not be sufficient to crush them. Figure 2.5 compares the strength of different proppant types.

2.8.2. Proppant Types

The various types of proppants used in the industry include sand, ceramics or carbides, polymer-coated / resin-coated particles, and hollow glass spheres. Fibers are sometimes added in fracturing fluids, not necessarily to act as proppant, though it can mechanically bridge fractures, but to impact the rheology of the fluid and reduce the rate of proppant settling.

2.8.2.1. Sand (Frac Sand)

Also known as silica sand, this is the most frequently employed proppant type due to its economic benefits. It constitutes processed and graded quartz sand with a high silica content. Frac sand comes in two primary types: white sand and brown sand. Brown sand, having a higher impurity content than white sand, is more susceptible to crushing at lower stresses. Consequently, brown sand is more cost-effective than white sand.

2.8.2.2. Ceramic Proppants

Produced from sintered bauxite, kaolin, magnesium silicate, or combinations of bauxite and kaolin, ceramic proppants offer greater benefits than silica sand. This is evident in their higher strength and greater crush resistance, more consistent size and shape, increased sphericity and roundness. Generally, they exhibit superior conductivity under specific closure stress conditions compared to other proppants. Also, they stand out for their superior chemical and thermal stability. However, their downside lies in their costliness and their potential to expedite the degradation of oxidizing breakers, hastening gel viscosity reduction and proppant settling.

Per their density, ceramic proppants are categorized as—lightweight ceramics (LWC), intermediate density ceramics (IDC), high-density ceramics (HDC), and ultra-high-strength proppants (UHSP). The alumina content directly correlate with both the proppant density and strength.

2.8.2.3. Resin-Coated Proppants (RCP)

Resin systems are typically produced from a reactive polymer and a curing agent or hardener. The coating is employed on sand, glass beads, and ceramic proppants; mainly serving as a trap for fragments of broken grains within the coating, thus preventing proppant flowback to the wellbore. Another application involves the prevention of sand production in soft formations. However, a

notable drawback of this technology is the low softening or degradation temperatures, attributed to the resin's polymer-based composition.

Kolawole et al (2019) noted that under realistic downhole fracture conditions with or without cyclic stress, curable resin-coated sand generates fewer fines compared to uncoated frac sand and lightweight ceramic (LWC). This was confirmed through tests under various conditions of fracture gradient, proppant weight, pump injection rates, and fluid density. For a consistent closure stress and temperature, analysis of 16 Bakken wells that underwent hydraulic fracturing showed that curable resin-coated sand treatments produced 27 lbm/billion fines, uncoated frac sand treatments produced 47 lbm/billion fines, and LWC treatments produced 97 lbm/billion fines.

2.8.2.4. Ultra-lightweight proppants

These aid in minimizing proppant settling, enhancing distribution within the fracture, and, when used with low fluid viscosity, contribute to an extended propped length. Lightweight proppants are the preferred choice in shale reservoirs because they can be effectively transported by the low-viscosity slick water commonly employed as the fracturing fluid in this type of formation, unlike high-density proppants.

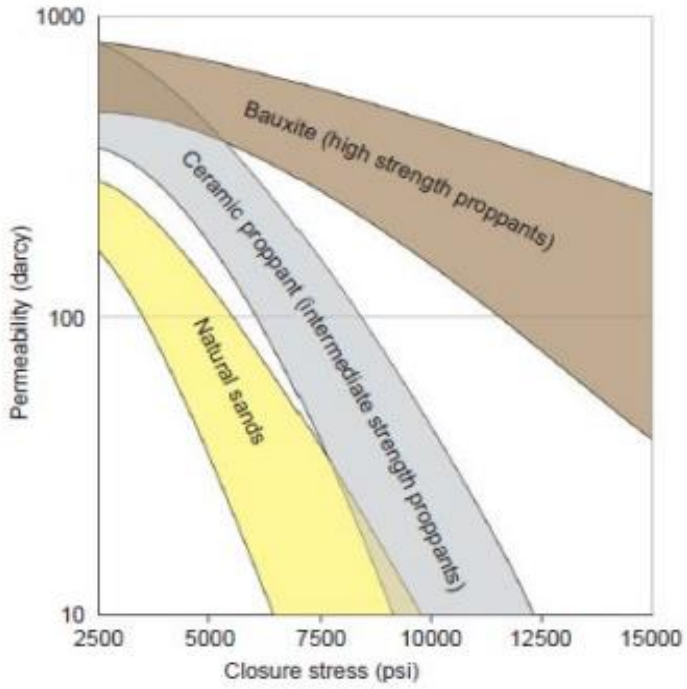

Figure 2.5 Comparison of strength of different Proppant Types (Bellarby, 2009)

The above figure (2.5) suggest that various proppant types can be identified by the following closure stress ranges:

- Sand: maximum of 6000 psi
- Resin-coated proppant: maximum of 8000 psi
- Intermediate-strength proppant (ISP): ranging between 5000 psi and 10000 psi
- High-strength proppant: closure stresses at or exceeding 10000 psi.

2.9. Rheology of Particle-Laden Fracturing Fluids

The viscosity of a fluid tends to increase when particles are introduced, primarily due to heightened viscous dissipation at the no-slip boundary surrounding each particle. This phenomenon is well-explained in Newtonian fluids through equations (9) formulated by Einstein and Batchelor.

$$\frac{\eta}{\eta_s} = 1 + \frac{5}{2}\Phi + C_2\Phi^2 \qquad (9)$$

Where the constant C_2 is dependent on the type of flow and the Peclet number (Barbati et al, 2019).

In the case of suspensions, viscosity reaches its peak at maximum packing fraction, and the rheological characteristics are influenced by factors such as particle size distribution. Notably, fiber dynamics deviate significantly from those of spheres. In dilute and semidilute regimes, fiber suspensions exhibit distinct rheological behaviors, shaped by aspects like aspect ratio, concentration, and fiber length. Shear thickening, characterized by a rise in viscosity with shear rate, is observable in certain fracturing fluids, particularly at concentrations exceeding 40% solid particles. Describing the rheology of non-Newtonian fluids laden with particles is intricate, with viscoelastic effects often accentuated in the presence of solids. Research delves into the non-Newtonian rheology of suspensions within yield-stress fluids, presenting promising yet challenging extensions of Newtonian findings.

2.10. Hydraulic Fracture Modeling

In selecting an appropriate model, the availability and quality of input data must be critically assessed. Notably, hard data like pad volume, injection rate, propping agent type, well completion details, fracture fluid viscosity, fracture fluid density, treatment volume, and propping agent volume can easily be controlled for optimal output. However, soft data involving in-situ stresses,

formation porosity, Formation depth, formation modulus, reservoir pressure formation permeability, formation compressibility, and reservoir thickness cannot be controlled. The dominant processes that must be captured in hydraulic fracture modeling include:

a. Fracture geometry creation
   Pore pressure, elastic and plasticity of formation
   Assumptions in the model, rock shear and slip

b. Fluid leakoff
   Pressure-dependent leakoff highlights fluid loss with increasing fracture pressure.
   Whole gel leakoff involves the loss of fluid as whole gel rather than as individual fluid particles.

c. Fluid rheology
d. Proppant transport

It is required for the selected model to include the basic physics of all significant processes. Also, it must have the ability to mimic and predict job results as well as provide decision making capability.

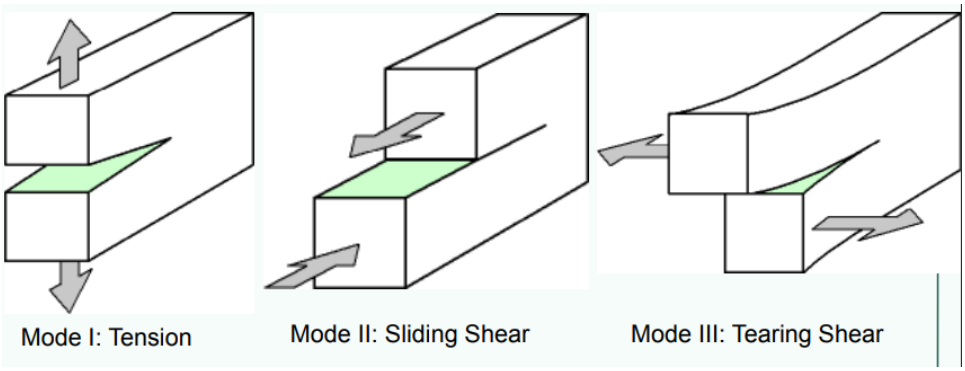

Figure 2.6 Modes of Fracture (Failure mechanisms)

Figure 2.6 above depicts the primary modes of fracture in a formation. Mode I depicts a pure tensile opening, recognized and addressed solely by conventional linear-elastic fracture mechanics (LEFM) models. Model II characterizes shear failure through sliding in the direction of the applied load and Mode III fracture is the tearing or lateral out-of-plane shear mechanisms.

2.11. Fracture Models

All hydraulic fracturing models have the fracture propagation as a function of injection of fracturing fluid, denoted as Q, originating from the injection line or point representing the perforations of the well. Consequently, it is assumed that a bi-wing symmetric fracture will propagate within the formation, perpendicular to the minimum principal stress of the formation. The generated fracture width is thus influenced by effective stress, defined as the difference between pore pressure and the minimum principal stress. Effective pressure serves as a reliable indicator of fracture width and is likely to correlate with well performance post-hydraulic fracturing. Higher effective pressure recorded during hydraulic fracturing is indicative of anticipated improved well productivity.

Available fracture models are classified as 2D models, Pseudo-3D models, Lumped parameter models, and 3D models.

2.11.1. Two-dimensional (2D) Fracture Models

2D fracture models are simplistic and captures the rudimentaries of hydraulic fracturing. There are primarily three of such models: Perkins – Kern Nordgren (PKN); Khristianovich -Geertsma-DeKlerk (KGD) and Penny-shaped fracture model. These models are with the assumption that the formation is homogenous and isotropic, and the fracturing process reveals a symmetric, bi-wing fracture from the injection fluid's point of line source.

2.11.1.2. PKN Model

The Perkins and Kern (PKN) model postulates a constant fracture height, irrespective of the fracture length. In this model, a two-dimensional plane-strain assumption is made in the vertical plane, where the fracture exhibits an elliptical cross-section in both horizontal and vertical directions. The model presupposes a fracture height significantly less than the fracture length. Additionally, it assumes that the hydraulic fracturing energy introduced by fluid injection is exclusively dissipated through energy loss from fluid flow, emphasizing a viscosity-dominated

regime, while disregarding fracture toughness. Figure 2.7 below illustrates the schematic representation of fracture geometry in the PKN model.

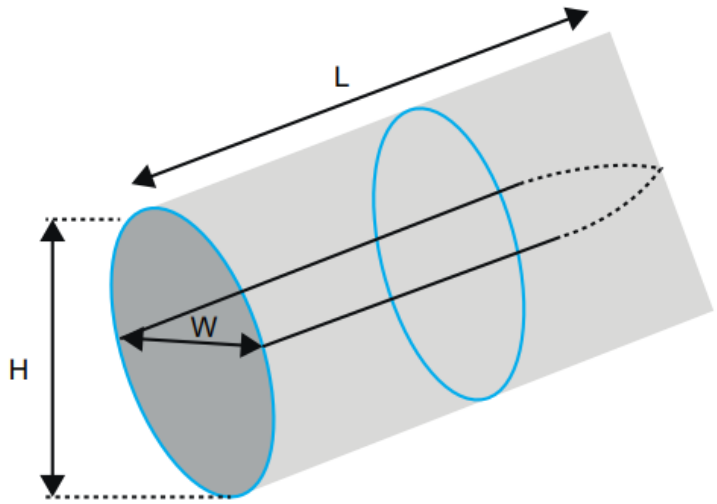

Figure 2.7. PKN Fracture Geometry Model (Hoss et al, 2017).

2.11.1.3. KGD Model

The KGD model is based on a two-dimensional plane-strain concept within a horizontal plane. Unlike PKN model, it features a constant fracture height exceeding the fracture length. This model assumes an elliptical horizontal cross-section and a rectangular vertical cross-section, where the fracture width is independent of the fracture height, persisting in a uniform manner (constant) vertically. The rock stiffness is exclusively taken into account in the horizontal plane. Figure 2.8 depicts the KGD model of a fracture geometry.

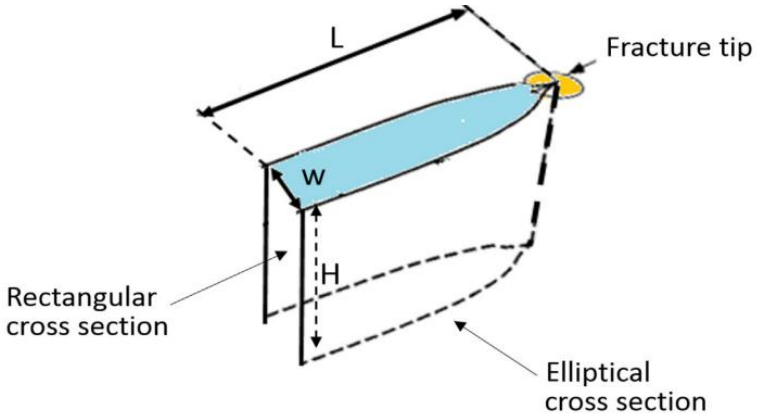

Figure 2.8. KGD Fracture Geometry Model (Hoss et al, 2017).

It is worth noting that both KGD and PKN models assume the flow of fluid in a fracture as a 1D problem in the direction of fracture length or fracture propagation. This is regulated by the Poiseuille's law and lubrication theory. Both models presume the fracture is enclosed and the horizontal stress, and reservoir temperature and pressure remain constant.

2.11.1.4. Penny-shaped fracture model

Also known as radial model, the Penny-shaped 2D model assumes the symmetric geometry to be at the line or point of injection source. Here, both fluid pressure and rate of injection within the fracture are assumed to be constant. Figure 2.9 below is an illustration of this type of model. They are usually applied in shallow formations where the minimum horizontal stress and overburden stress become equal.

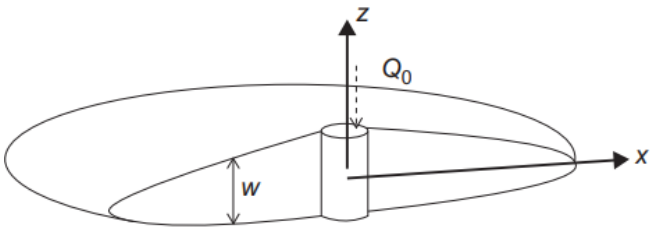

Figure 2.9. Fracture geometry of the penny-shaped model, (Hoss et al, 2017).

2.11.2. Pseudo-3D (P3D) Hydraulic Fracturing Models

For practical purposes, P3D models serve as better alternatives to 2D models. This is because they consider fracture heigh variation as a function of location in time and fracture propagation direction. Here, the equilibrium and dynamic height pseudomodels are introduced. Equilibrium height pseudomodels assume that the fracture height will eventually reach an equilibrium state, where the fracture no longer propagates upwards. At this point, the pressure within the fracture is assumed to be uniformly distributed across the entire height of the fracture. The dynamic height psudomodels take into account the fact that fracture height can change over time. They assume 2D fluid flows, that is, perpendicular and parallel to fracture path. This is in contrast with 2D models, where fluid flow is in 1D along the fracture path. Also, in P3D models, toughness criteria for the propagation of fractures are considered. Fracture toughness here refers to the stress intensity factor required to cause the fracture to propagate. P3D models are demerited by their restrictions to certain geometries and their underlying plane-strain conditions in every cross-section perpendicular to the path of fracture. They also provide different accuracies in different fracturing regimes. Particularly, they are not accurate enough n both toughness dominated and viscosity dominated regimes due to their local elasticity assumption and viscous losses perpendicular to the path of fracture. Figure 2.10 illustrates this fracture model. Examples of P3D models include MFRAC, StimPlan, e-StimPlan and FracCade.

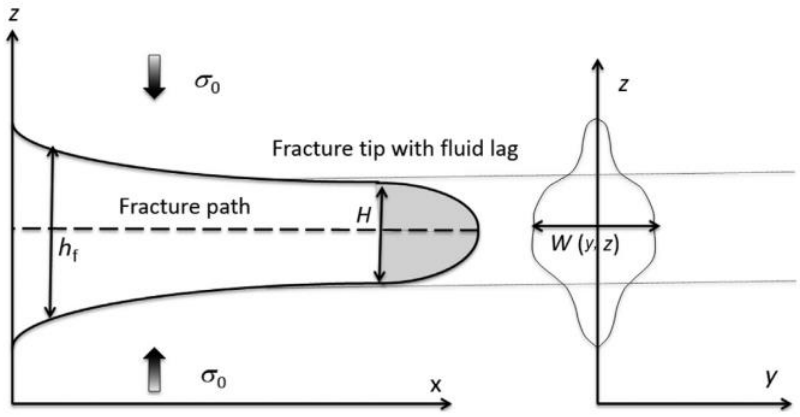

Figure 2.10. P3D fracture model (Hoss et al, 2017)

2.11.2.1. Lumped Parameter models

Lumped parameter models like FracPro and FracPro-PT characterize fracture growth solely at three specific locations: the upper, lower, and lateral tips of the fracture. Consequently, the fracture is assumed to be of a 'semi-similar' elliptical shape, defined by connecting these identified points. Within this model, fracture growth is influenced by vertical and horizontal pressure gradient functions. The outcome is a projected fracture that is notably wide with a relatively short length, primarily caused by user-controlled input functions rather than measured properties of rock. An illustration of a lumped parameter model is presented in Figure 2.11.

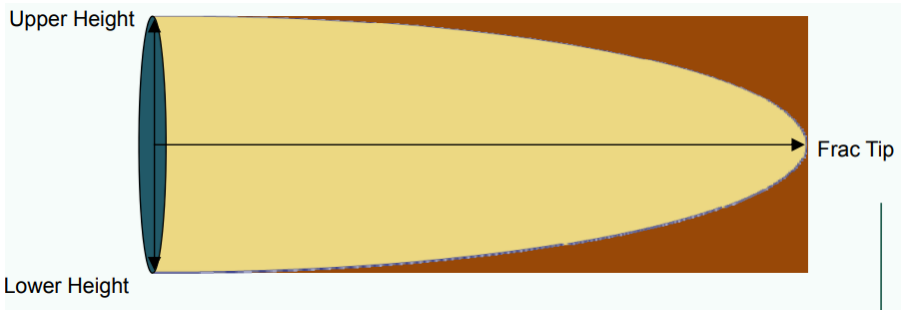

Figure 2.11. Lumped parameter fracture model (R.D. Barree)

2.11.3. Three-dimensional (3D) Fracture Models

Complete 3D models necessitate the solution of sets of coupled partial differential equations that govern multiphase fluid flow in fracture, rock deformation, and leak-off. To mitigate computational expenses, simplified models have been introduced, incorporating one-way or weak coupling. The simulation of hydraulic fracturing encounters additional challenges due to the intricate dynamics of fluid lag and fracture-tip behavior. A conventional approach for simulating fracture propagation is the Displacement Discontinuity (DD) method, which is a modification of the boundary element method. Various finite element methods have also been employed in hydraulic fracturing simulation. Compared to the DD method, finite element methods offer greater flexibility, as they do not mandate explicit calculations of the kernel function.

Notable fracture 3D models include N-StimPlan, Terra-Frac, and GOHFER®. The N-Stimlab model employs a gridded width and flow solution akin to GOHFER® and depends on a linear-elastic coupling of the rock. Terra-Frac, on the other hand, utilizes a triangular mesh finite element width solution with fully coupled stress intensity factor and elastic deformation tip conditions. However, it is constrained to a single fluid injection point and necessitates re-meshing over time.

The GOHFER® model adopts a gridded deformation solution and aims to predict the anticipated discontinuous nature of rocks, accounting for bedding planes, incipient failure or planes of weakness, and pre-existing natural fractures and fissures. Notably, it incorporates a shear-decoupled formulation of fracture, acknowledging that shear failure and slip commonly occur during hydraulic fracturing operations. Consequently, GOHFER® is considered one of the most dependable fracture simulators. Furthermore, it features a comprehensive database of fluid rheology and proppant transport models extensively validated through laboratory research.

2.12. Effective Stress

Tectonic stress, fluid pressure and overburden pressure all influence fluid-saturated reservoir rocks. One essential reservoir property is the permeability of the rock. While some researchers argue that this rock property is solely dependent on effective stress, others propose a more nuanced viewpoint. This perspective suggests that both confining pressure and pore pressure have an impact on permeability, however, it is more significantly influenced by pore pressure (Zoback et al. 1975).

Effective stress is mathematically defined by equation 10 as:

$$\sigma_{e} = \sigma_{n} - \alpha P \tag{10}$$

Where: σ_e is effective stress, α represents the Biot's poroelastic coefficient and σ_n denotes the overburden pressure, which is usually the normal stress applied to the rock.

The flowing bottomhole pressure, which occurs within the wellbore during flow conditions, holds significant importance as the stress on the proppant is dependent on both closure pressure and flowing bottom-hole pressure. Any fluctuation in flowing bottom-hole pressure prompts a re-arrangement of proppants (distribution) within the fracture, potentially resulting in a loss of conductivity. Figure 2.12 illustrates an ideal and actual proppant placement during hydraulic fracturing and subsequent well production. While an ideal scenario assumes a uniform proppant distribution within the fracture, practical considerations such as proppant settling velocity and fluid leak-off to the formation introduce non-uniformities, creating propped and unpropped regions within the hydraulic fracture. The unpropped region undergoes closure, and the fracture width in

the propped region decreases due to an increase in effective stress during production, ultimately leading to a reduction in fracture conductivity.

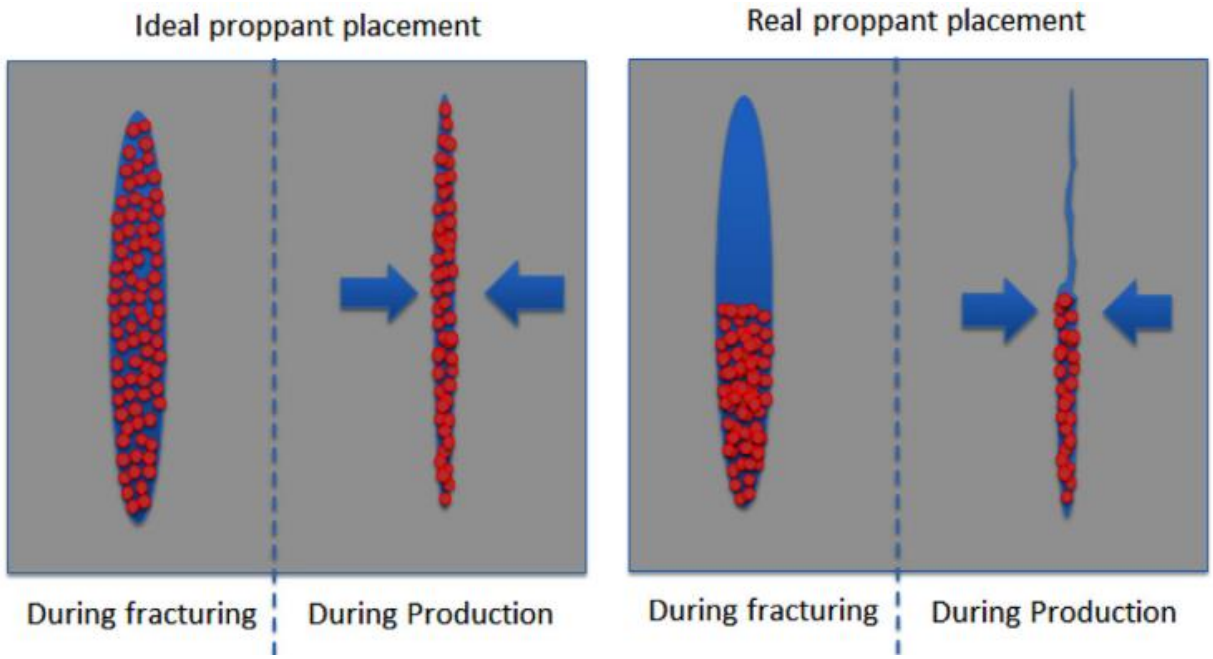

Figure 2.12. Ideal and Actual Placement of proppants in hydraulic fracturing. (Hoss et al, 2017)

Rozhko et al (2011) explored the theory of effective stress with capillary action. It was explained that the interaction of fluids with rocks affects their (rocks) strength and deformability through processes like mineral dissolution and osmotic diffusion. Capillary effects arise when pore space is partially saturated with immiscible fluids, influenced by surface tension and wettability. The remarkably low permeability found in tight and ultra-tight formations, combined with the narrow natural and created fracture widths from such fluids as slickwater, emphasizes the significant role of capillary forces during the production phase. The introduction of water through injection is reported to create capillary barriers that result in decreased production rates. Additionally, the reduction in permeability near the fracture face, attributed to clay swelling and the infiltration of polymeric fluids into the formation, further compounds these challenges.

The relationship between effective stress and hydraulic fracturing propagating pressure in clastic reservoirs was also examined by Pater et al (2017). In their study, net pressure correlated well with effective stress, indicating its significant role. Stress shadow was also noted, altering the stress regime surrounding propagating fractures.

2.13. Stress Shadow

Created fractures disrupt the surrounding stress distribution, which consequently impedes the advancement of other developing fractures. This disruption is referred to as the "stress shadow" phenomenon. In terms of measurement, within a horizontally fractured well, stress shadowing becomes evident through a rise in the in-situ stress aligned with the wellbore. A significant factor influencing the asymmetric growth of hydraulic fractures is stress shadow. Similar to the impact of depletion, which can generate uneven stress around a wellbore, stress shadows also induce non-uniform and frequently asymmetric alterations in the stress field. Consequently, the resultant uneven stress field can result in asymmetric growth of fracture wings, both laterally and vertically. The figure 2.13 below illustrates the limiting impact of stress shadow on fracture creation and propagation.

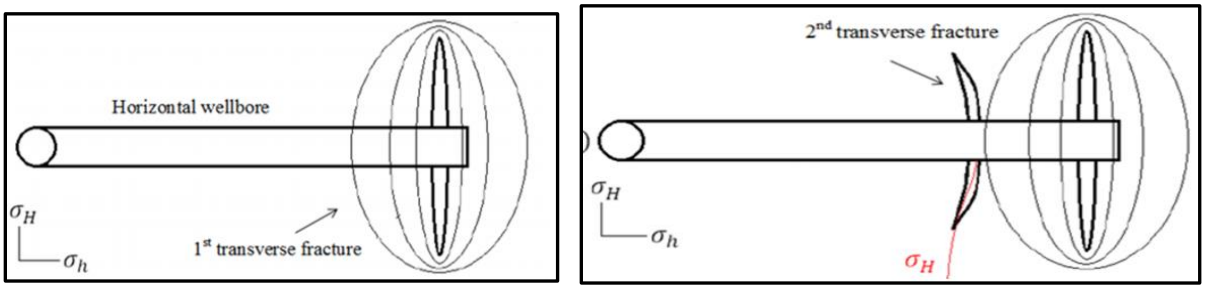

Figure 2.13. Stress shadow altering the propagation of immediate fracture (right).

Stress shadows, fracture geometry, proppant selection, and fracturing fluids' properties all contribute to the complexity of hydraulic fracturing in unconventional reservoirs. Understanding and managing these factors hold the key to achieving optimal hydraulic fracturing outcomes, enhancing productivity and sustainability in the energy industry.

2.14. Hydraulic Fracture Properties

2.14.1. Fracture Half Length

Fracture half-length, known as xf, is crucial in the deliverability of hydrocarbons from the reservoir to the fracture, which is often balanced with the flow of these hydrocarbons from the fracture to

the wellbore, (typically characterized by FC, the fracture conductivity) for optimized hydrocarbon production. Reservoir contact, which directly affects production, relies on various elements such as lateral length, stage count, fracture height, and fracture half-length. Fracture height and fracture half-length can be controlled by manipulating fluid rate, volume, and viscosity during hydraulic fracture treatments.

Various studies have explored the optimal combination of fracture attributes in relation to the reservoir conditions. Notably, it has been established that exceptionally high fracture conductivity may not be a universal requirement for all types of reservoirs. In the case of extremely low-permeability reservoirs, where hydrocarbons struggle to traverse the tight reservoir rock, the primary focus shifts towards achieving a long effective fracture length rather than simply maximizing flow capacity along the fracture. However, even in these scenarios, fracture conductivity remains a crucial factor. To ensure an extended effective fracture length, the fracture must maintain a level of conductivity that facilitates the efficient retrieval of fracturing fluids while minimizing damage to the formation and proppant pack.

Indeed, the significance of fracture half-length becomes even more evident when considering gas production in shale formations. It is widely recognized that longer fracture half-lengths, coupled with shorter fracture spacing, lead to higher gas production rates. This is because a greater number of fractures in the shale surrounding the wellbore accelerates the release of gas. Yet, it is essential to note that while initial production may increase linearly with the number of fractures, sustaining a high gas flow rate becomes challenging as fractures begin to interfere over a given lateral length.

2.14.2. Fracture Conductivity

Fracture conductivity plays a pivotal role in increasing reservoir contact and optimizing flow capacity, both of which are vital for boosting production. The permeability and conductivity of proppant undergo alterations in response to various stress conditions. For instance, the permeability of 20/40 mesh, and consequently the conductivity, exhibit variations between 6000 psi and 10,000 psi of closure pressure. It typically decrease with closure pressure (Hoss et al, 2017).

The true essence of fracture conductivity lies in its ability to sustain efficient hydrocarbon flow. This is predominantly governed by two critical factors: proppant volume and proppant selection.

Fracture conductivity (Cf), also known as flowback capacity, is quantified in md-ft units and is expressed as a function of fracture permeability (kfrac) and fracture width (wfrac), represented by the equation 11 below:

$$C_f = k_{frac}\, x\, w_{frac} \tag{11}$$

In essence, it quantifies the ease with which fluids can move through the fracture network.

To measure and compare fracture conductivity, industry standards like the International Organization for Standardization (ISO) and the American Petroleum Institute (API) have established guidelines. The ISO-13503-5 standard outlines long-term conductivity testing procedures (baseline conductivity), while the API-RP-19D standard also adopted these guidelines in 2008.

In practical terms, fracture conductivity serves as the lifeline of drilling and completion operations in unconventional plays. Without a sufficiently conductive pathway for hydrocarbons to flow through fractures to the wellbore, all efforts in these operations may go to waste. Therefore, understanding, quantifying, and optimizing fracture conductivity is essential for maximizing production and reservoir performance in unconventional oil and gas reservoirs.

2.15. Fracture Treatment Design

2.15.1. Pre-treatment Evaluation of Formation

Prior to conducting hydraulic fracturing treatment, a thorough analysis must be made to reach a great understanding of the reservoir. This involves:

a. *Geological analysis* to determine such formation characteristics as the lithology, clay content, fault patterns, drainage area, and radius. Understanding geologic deposition patterns and drainage area is crucial, as engineers need to determine optimal values for fracture lengths and drainage radius. The selection of hydraulic fracturing fluid is influenced by the reservoir's lithology. Also, analyzing regional and local fault systems allows for the investigation of in-situ stresses in rocks.

b. *Well-logging analysis* to determine water saturation, rock mechanical properties, net pay thickness, permeability and porosity of the formation. Data from logs also enable the estimation of shale content, oil and gas reserves

c. *Core analysis* for correlation between log and core measurements. Also for porosity and permeability determination and for evaluation of oil or gas in place.

d. *Well testing*: The primary goal of a well test is to identify dynamic reservoir permeability, skin factor, initial reservoir pressure, in-situ stresses, and effective fluid loss. Additionally the potential flow of reservoir can be observed.

2.15.2. Design

The concept underlying an optimal fracture design is to achieve maximum reservoir yield with cost being kept minimal. The most effective and thorough design emerges from an analysis of completed wells, comparing the data with their production performance. It is imperative that the chosen completions design for the well is guided by the production performance of the well.

Broadly, the design of hydraulic fracturing treatments relies on information gathered during pretreatment formation evaluation to optimize the net present values (NPVs) of fractured wells. Proper planning of fracturing fluid and proppant specifications, fluid volume, proppant weight requirements, injection schedules, mixing schedules, and predicted injection pressure profiles is essential before initiating field operations.

2.15.2.1. Parameters To Consider

2.15.2.1.1. Clean Volume and rate

This signifies the fluid volume composed solely of water and chemicals. Clean rate" denotes the rate of the clean side (water and chemicals).

2.15.2.1.2. Slurry volume and rate

This encompasses combinations of water, sand, and chemicals. Slurry rate represents the rate of the slurry (water, sand, and chemicals). It is typically is obtained from a flow meter situated on the

blender. The volume of fluid slurry per stage at various proppant concentrations can be calculated and is included in the frac schedule provided to field personnel.

2.15.2.1.3. Absolute Volume Factor

The Absolute Volume Factor (AVF) pertains to the total volume occupied by a solid within water. It is contingent upon the density of the frac fluid and the specific gravity of the proppant employed.

2.15.2.1.4. Stage proppant

The stage proppant refers to the quantity of proppant needed at different proppant stage concentrations. For instance, at a proppant concentration of 2 ppg, the stage proppant could be 40,000 lbs of sand, contingent on the clean volume. It is determined by the proppant concentration and the clean volume of the stage fluid.

2.15.2.1.5. Stage fluid clean volume

Stage fluid clean volume denotes the quantity of clean volume allocated for each proppant stage concentration. The determination of clean volume for each proppant stage concentration is based on the desired contact surface area. The volume of water to be pumped is also influenced by factors such as water availability, formation properties, transportation convenience, well spacing, and the proximity to adjacent producing wells. In certain instances, to minimize fracture communication between newly drilled wells and existing production wells in a given area, the amounts of both sand and water are reduced. This reduction is implemented to prevent fracture interference, a phenomenon also known as "frac hit."

2.15.2.1.6. Slurry density

Slurry density pertains to the density of the water and sand being injected downhole. It directly influences the hydrostatic pressure within the casing during a frac job, with an increase in slurry density corresponding to an elevation in hydrostatic pressure. When exclusively water is pumped downhole, the hydrostatic pressure of the water column can be determined using the hydrostatic pressure equation. However, when various sand concentrations are introduced at different stages of hydraulic fracturing, slurry density becomes a crucial factor in hydrostatic pressure calculations.

2.15.2.1.7. Sand-to-water ratio

Calculating the total sand divided by the total water per stage provides the sand-to-water ratio. A lower ratio indicates a higher percentage of water compared to sand, while a higher ratio suggests

more aggressive stages with a greater amount of sand relative to water. In slick water fracs, the sand-to-water ratio typically falls within the range of 0.7 to 1.7. However, in more viscous fluid systems like cross-linked jobs, the sand-to-water ratio can be significantly higher.

2.15.2.2. Slickwater Fracturing Treatment Schedule

The horizontal well is segmented into numerous stages, and the number of stages is contingent on the lateral length. Generally, an increase in lateral length corresponds to a higher number of stages.

In slick water frac operations, each stage may utilize proppant ranging from 150,000 to 800,000 lbs. The proppant stage concentration typically begins with a low concentration, ranging from 0.1 to 0.25 ppg. The clean volume for each proppant stage concentration can vary. The average water volume per stage is influenced by various design factors such as treatment complexity, sand quantity, stage length, and more. Typically, a stage in slick water jobs can require anywhere from 4,000 to 14,000 BBLs of water. In cross-linked jobs, the demand for water is reduced since the high-viscosity fluid effectively transports the slurry into the formation.

2.16. Production Forecasting and Economic Analyses

A final design is reached upon the basis of production forecast and economic analysis, most especially, net present value (NPV) analyses. The dimensionless fracture conductivity becomes essential in doing this. It quantifies the relative ease with which fluids can flow through the propped fracture in comparison with the surrounding reservoir rock. Thus, it is used to assess whether the created fracture provides adequate flow conductivity to enhance well productivity. Generally, a high dimensionless fracture conductivity is desired. Equation 15 illustrates the mathematical expression. Figure 2.14 also depicts the characteristics of a two-stage hydraulic fracturing process and the stimulated reservoir volume that are crucial parameters for determining the dimensionless fracture conductivity (FCD).

$$F_{CD} = \frac{K_f \, x \, w}{K \, x \, X_f} \tag{15}$$

Where: K_f is fracture permeability in mD, w is fracture width in ft, K is fracture permeability in mD, X_f is fracture half-length in ft and F_{CD} is dimensionless fracture conductivity.

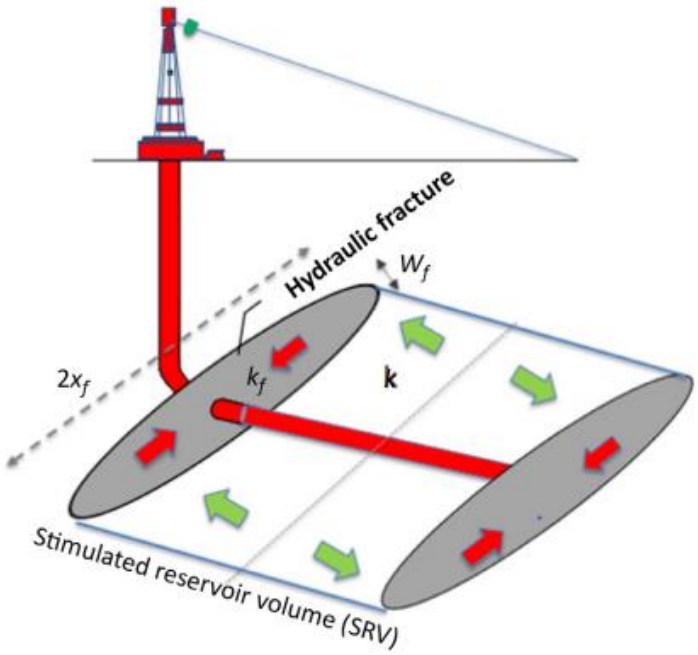

Figure 2.14. Parameters involved in determining FCD in a two-staged hydraulically fractured horizontal well

By comparing the expected production of a fractured well to the projected decline in production of the unstimulated well, the additional production that can be attributed to the fracturing treatment can be estimated. This incremental production is then used to calculate the annual economic benefit of the fracturing job. Mathematically:

$$\Delta N_{p.i} = N_{p.i}^{f} - N_{p.i}^{nf} \tag{16}$$

Where: $N_{p.i}^{if}$ is the forecasted annual incremental cumulative hydrocarbon recovery of non-fractured well for year i (ft^3), $N_{p.i}^{f}$ is the forecasted annual incremental cumulative hydrocarbon recovery of the fractured well for year i (ft^3) and $\Delta N_{p.i}$ is the predicted annual incremental cumulative hydrocarbon recovery for year i (ft^3).

The incremental revenue and net present value of the fracturing project can then be estimated based on the results.

2.17. Geologic Background for the Study

The Marcellus Shale is a vast and prolific geological formation located primarily in the Appalachian Basin of the Eastern United States. It is one of the most significant sources of natural gas in North America and it stretches across multiple states, including Pennsylvania, West Virginia, Ohio, and New York.

Geologically, the Marcellus Shale is a sedimentary rock formation that was deposited around 380 million years ago during the Devonian Period. It is composed of organic-rich mudstone and shale layers, and it was formed in a shallow marine environment. Over time, the organic material present in the shale was transformed into hydrocarbons through heat and pressure, leading to the accumulation of natural gas within the rock.

With characteristics like permeability ranging from 0.001 md to 0.0001 md, porosity of 2-10%, average Young's moduli, low Poisson's ratio and stress anisotropy, the Marcellus shale becomes a suitable candidate for single and multi-stage hydraulic fracturing. It remains a complex unconventional reservoir that does not respond in a straightforward manner during large scale hydraulic fracture stimulation. Completion efficiency along the lateral is affected by preexisting fractures oriented at an angle to existing principal stresses and strongly influence hydraulic fracture propagation.

2.17.1. MSEEL

MSEEL, fully named the Marcellus Shale Energy and Environment Laboratory, is a research project that provides a long-term collaborative field site to develop and validate novel knowledge and technology. Ultimately, the initiative seeks to enhance recovery efficiency and mitigate environmental implications of unconventional resource development.

The MSEEL wells are in the core play area of the Marcellus Shale in Monongalia County, West Virginia. The initial well site is situated within the Morgantown Industrial Park (MIP) area in West Virginia, USA. Operations at this location commenced during the autumn of 2015 with the drilling of the Northeast Natural Energy MIP-3H and MIP-5H wells, alongside the vertical MIP-SW well designated for scientific and microseismic observation. Additionally, data from two previously

drilled lateral wells, MIP 4H and MIP 6H, which were drilled in 2011, are also harnessed as valuable data sources.

The Boggess site is the second and latest MSEEL site. Comprising six lateral wells and one vertical pilot well, as seen in figure 2.15. The Boggess site forms the primary focus of this study. A vertical model of the reservoir was constructed based on a core sample and an extensive suite of logs collected from the vertical pilot-hole of Boggess 17H. For better understanding of the lateral aspects of the reservoir, logging while drilling (LWD) acoustic imaging and acceleration logs were acquired from all the laterals except the 17H. A permanent fiber optics cable was installed in Boggess 5H lateral, while a retrievable fiber-optic cable was deployed in the Boggess-1H during the stimulation of Boggess 5H and 9H laterals. These fiber-optic cables facilitated the collection a set of distributed temperature sensing (DTS), distributed acoustic sensing (DAS), and microseismic data during completion of the 5H and 9H.
For this study, only the Boggess 5H lateral data and Boggess 17H vertical data were considered.

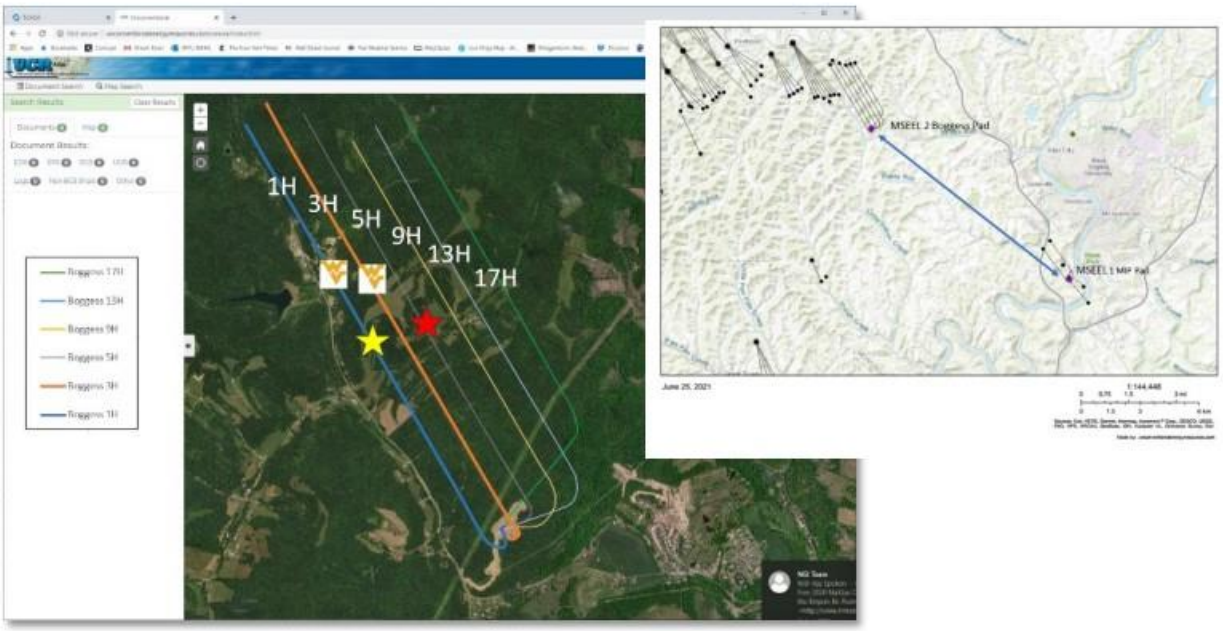

Figure 2.15. Location map showing horizontal wells drilled to the Marcellus Shale. Images are from data available from the MSEEL web site map viewer (http://www.mseel.org/viewer).

CHAPTER 3: OBJECTIVES AND METHODOLOGY

3.1. Objective

The primary purpose of the study is to explore how fracturing fluid choice and stress shadow impact proppant transport and productivity of multi-staged fractured Marcellus Shale horizontal wells. In achieving this, the following procedures were undertaken:

- Data collection
- Model development and estimation of hydraulic fracture properties
- Prediction of production
- Optimization

3.1. Data Collection

Data required for this study was obtained from the MSEEL website, specifically from the lateral Boggess-5H well and the vertical section of the Boggess-17H well.

3.1.1. Well Log Data

This encompasses several log data including resistivity, density, gamma ray, neutron and acoustic log measurements. The sonic scanner log enabled the estimation of the pore pressure gradients while the density log was used to estimate the overburden stress and two elastic properties: Poisson's ratio and Young's modulus.

3.1.2. Core Data

Utilizing core plugs extracted from the Boggess 17H well, shale mechanical properties and adsorption traits were determined. Various tests such as triaxial compression and comparisons of multiple stress paths, were conducted. This allowed for the quantification of parameters such as shear modulus, Young's modulus, Poisson's ratio, all in normal and parallel orientations to bedding, as well as the measurement of bulk modulus and anisotropy index.

3.1.3. Acoustic Borehole Image Logs

Analysis was made on the image logs from Boggess 5H to determine the natural fracture density around the well.

3.1.4. Hydraulic Fracture Treatment Data

Boggess 5H well was stimulated with 56 fracture stages. These featured an average length of 159 feet, with 3 to 5 clusters present within each stage, along with 8 perforation shots per cluster. For the base model, the slickwater fluid system was employed in every treatment stage except the few stages for acid pump. The average treating pressure was 8452 psi at an average rate of 79.4 bpm. The average pump time was 2 hours and 9 minutes. Also, a combined total of 14,009,020 lbs of 100 mesh sand and 6,842,300 lbs of 40/70 sand was placed, making a total of 20,851,320 lbs, which is 95% of the designed volume. 92,828 gal of 7.5% HCl was utilized during the stimulation treatment.

For modeling purposes, two out of the 56 stages of clusters were ignored due to data inconsistencies. Python programming language was then used to clean the raw pump treatment data of the remaining 54 stages and were input into the fracture modeling software. An illustration of the results from the pumping treatment is seen in figure 16.

3.2. Model Development

3.2.1. Estimation Of Hydraulic Fracture Properties

GOHFER (Grid Oriented Hydraulic Fracture Extension Replicator), a planar 3-D geometry fracture simulator, was used to simulate the hydraulic fractures and predict their properties. The software encompasses an extensive array of tools that facilitate well completion design, analysis and optimization process for unconventional reservoirs. It is inherently built to account for stress shadow effects when needed. With data from the treatment well - Boggess 5H and the reference well - Boggess 17H, a fracture model was developed. The log-derived estimates of Young's modulus and Poisson's ratio were calibrated with the core measurements. Geosteering techniques were implemented to accurately position the horizontal section of the well within the intended zone. The minimum horizontal stress and process zone stress (PZS) were also determined by the

software through its innate ability to perform the necessary calculations. As previously mentioned, the processed fracture treatment data for each stage was incorporated into the model. In addition, treatment pressure predicted by GOHFER were matched against actual treatment pressure for increased model accuracy. Ultimately, fracture properties like fracture half length, fracture conductivity, proppant concentration and fracture height, were predicted for two scenarios – with the interference of stress shadow and without stress shadow effect. Figure 3.1. shows an example of pumping treatment simulated in the GOHFER software.

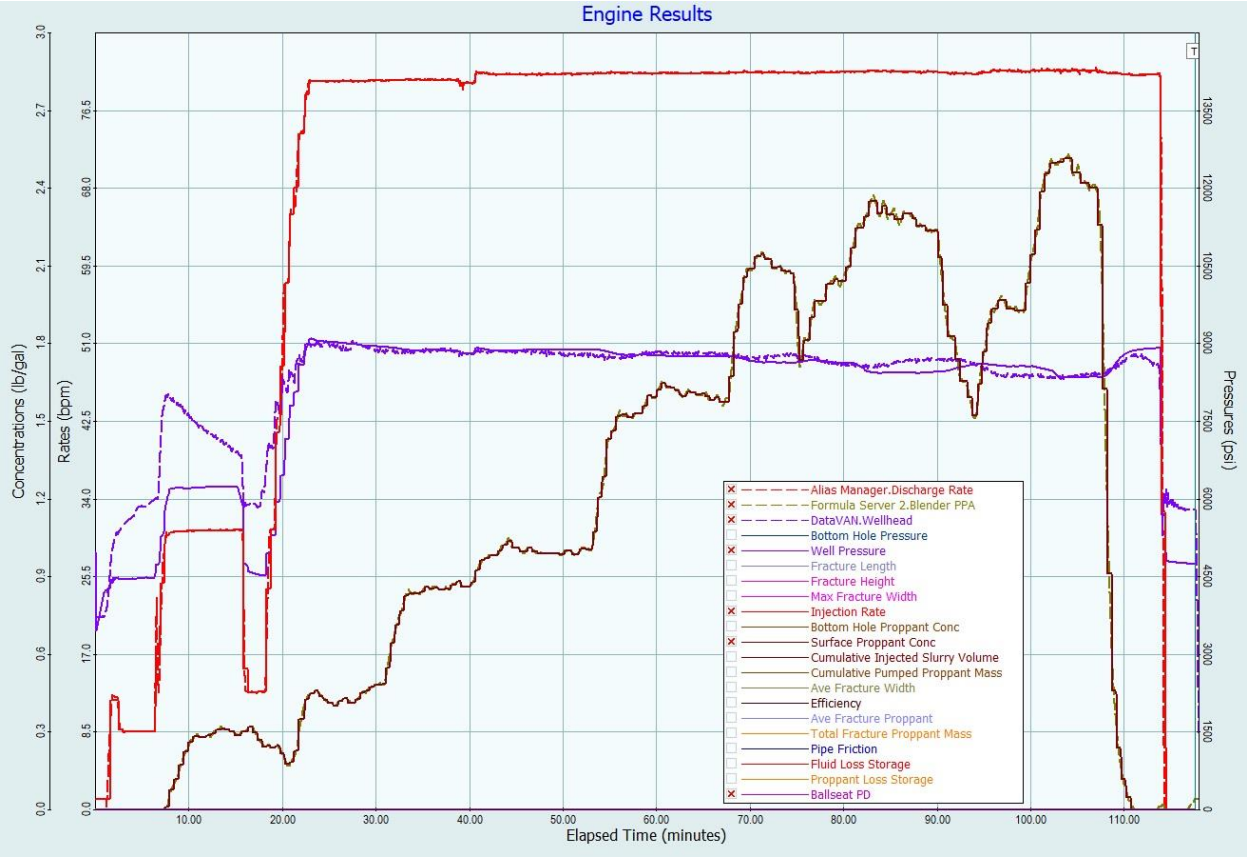

Figure 3.1 Graphical representation of Pumping Treatment for Stage 12 showing Slurry rate, Surface Pressure and Slurry concentration with time

3.2.2. Model Development for Predicting Production

To predict the production performance of the Boggess-5H well based on estimated hydraulic fracture characteristics, we employed reservoir simulation software (CMG-GEM, 2022). This software allowed the modeling of the reservoir as a dual permeability system, providing a precise and efficient means of simulating transient gas production from a horizontally fractured well within shale gas reservoirs. This modeling approach draws from the work of Rubin (2010) and Cipolla et al. (2010). Under this system, Gilman and Kazemi's methodology was utilized to simulate the flow from the matrix to the fractures. To enhance the accuracy of gas flow predictions from the matrix to the bi-wing hydraulic fractures, the local grid refinement (LGR) with logarithmic grid spacing was implemented. Additionally, the model accounts for non-Darcy effects in transient gas flow within hydraulic fractures.

To estimate the distribution of natural fractures or fissures, we relied on interpretations of acoustic borehole image logs, as previously discussed. The Langmuir constants for Marcellus shale were obtained through isotherm tests performed on crushed core plugs from the Boggess well 17. Furthermore, we incorporated multipliers for matrix permeability, fissure permeability, and hydraulic fracture conductivity, which were developed by El Sgher et al. (2018). These adjustments were made within the reservoir model to account for shale compaction resulting from the increase in net stress during production. Table1 shows the input parameters for the base model development.

Table 1. Reservoir Input Parameters

Reservoir Parameters	Values	Units
Model Dimensions (Boggess 3H)	13850 (Length)×1500(Width) ×100(Height)	ft.
Initial Reservoir Pressure	5200	psia.
Initial Fissure Porosity	0.1	percent
Initial Matrix Porosity	5.5	percent
Initial Fissure Permeability i, j, k	300,300, 30	nd
Initial Matrix Permeability i, j, k	450, 450, 45	nd
Water Saturation	0.15	Fraction
Rock Density	170	lb/ft3
Langmuir Pressure Constant	0.00149	psi-1
Langmuir Volume Constant	0.144	g-mol/lb

In order to mimic reality as closely as possible, geomechanical factors were incorporated into the model. Here, the impact of the change in the effective stress on permeability was accounted for by generating multipliers for matrix permeability, fissure permeability and propped fracture conductivity. **Figures 3.17, 3.18 and 3.19 are the graphical representations of these multipliers.**

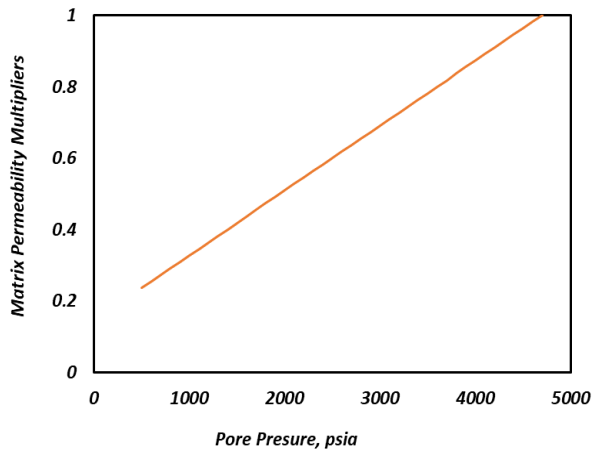

Figure 3.2 Matrix Permeability Multiplier

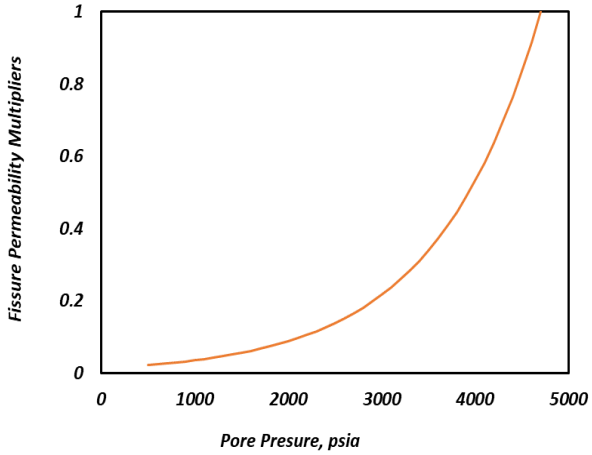

Figure 3.3 Fissure Permeability Multiplier

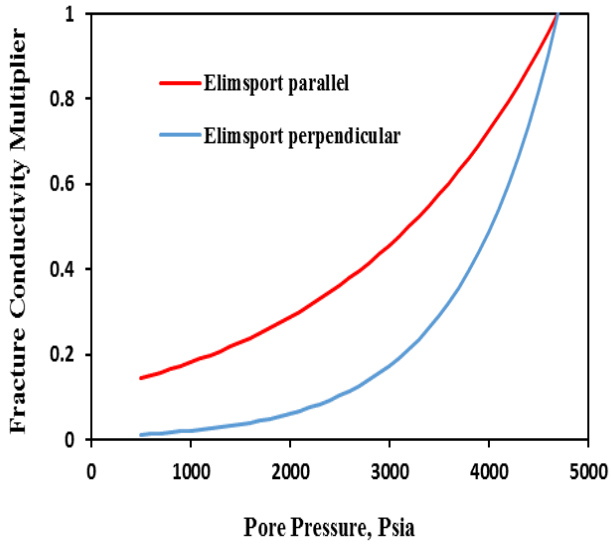

Figure 3.4 Propped Fracture Conductivity Multiplier

CHAPTER 4: RESULTS AND DISCUSSION

4.1. Model Credibility

The base model's credibility was confirmed by the close match between the actual production data and the predicted production**.** Figure 4.1 below illustrates a comparison between the gas production profiles generated using fracture properties, and the corresponding actual production data. The figure reveals that incorporating stress shadowing leads to a more accurate prediction.

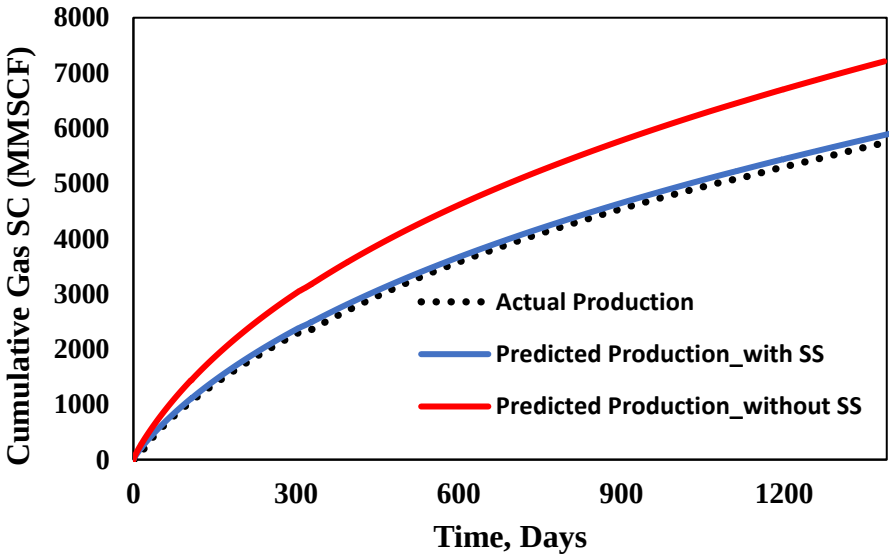

Figure 4.1 A Graph of Actual and Predicted Production data for Boggess 5H

4.2. Hydraulic Fracturing Prediction Results

Hydraulic fracture properties estimation and production prediction for the various fluids used in this study were done under two scenarios:

scenario 1: With stress shadow (SS) interference.

Scenario 2: Without stress shadow (SS) interference

Slickwater, which was the base fluid, was first used and fracture properties predicted. Afterwards, viscosity of the slickwater was improved by introducing the hybrid fluids. These hybrid fluids include:

a. Hybrid_1 = **75%** Slickwater and **25%** Flojet (8gpt)

b. Hybrid_2 = **75%** Slickwater and **25%** HyborGuar

Viscosity was further increased using 100 % Flojet (8 gpt) and 100 % Hybor Guar for further analysis. This sets the 100% fluids used for this study as:

a. Slickwater

b. Flojet (8 gpt), which is a high viscous friction reducer (HVFR)

c. Hybor Guar (Crosslinked Gel).

The effect of the various fluids on fracture geometry and production are discussed below.

4.2.1. Fracture Properties

4.2.1.1. Estimated Fracture Properties under Stress Shadow Effect

Table 2 below indicates the predicted average fracture properties for all fluids using the 3d GOHFER Software. Also, figures 4.2 - 4.6 are graphical representations of the estimated average fracture properties using the various fluids.

Table 2. Average Fracture Properties associated with the various fluid types (considering stress shadow effects)

Average	Slickwater	Hybrid_1	Hybrid_2	Flojet	HyborGuar
Avg. Fracture Half Length.ft	292.7368421	260.9323308	259.3082707	247.6240602	249.2932331
Avg. Fracture Height.ft	25.02828718	29.22863935	27.2902165	46.00889	43.36037504
Avg. Conductivity.md*ft2	4.275214883	4.827317256	4.656487816	3.757901019	3.803699023
Avg. Proppant Conc. Ib/ft2	0.543367795	0.552267559	0.541850246	0.567705361	0.566202041
Avg. Fracture width.ft	0.404961954	0.424299825	0.447679592	0.471327778	0.465920323

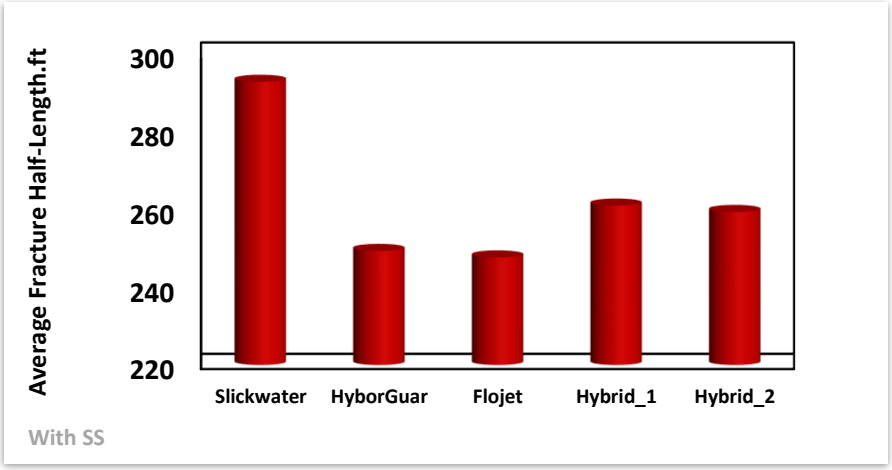

Figure 4.2 Average Fracture Half-Length for all fluid types with stress shadow effect

Slickwater exhibited the highest average fracture half-length when compared to the hybrid fluids with the average fracture half-lengths of the two hybrid fluids being roughly the same. Similar occurrence happened with the 100% fluids, where Slickwater gave the highest value and the two other fluids lagged behind with roughly the same values.

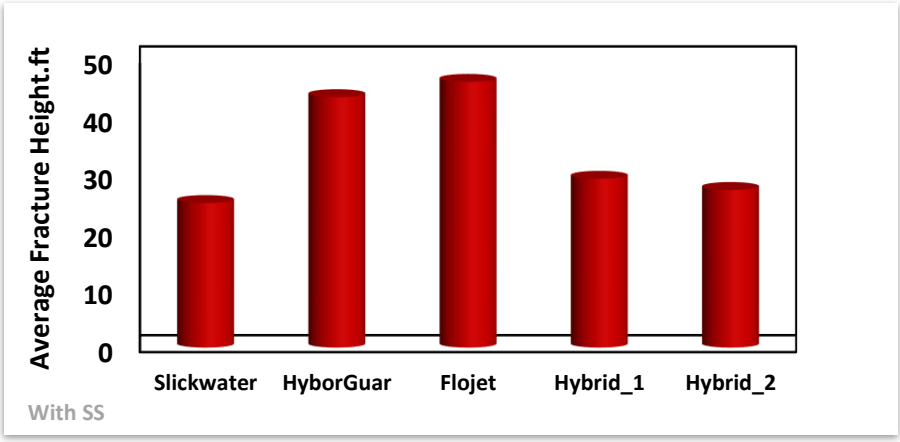

Figure 4.3 Average Fracture Height for all fluid types with stress shadow effect

Hybrid_1 produced the largest average fracture height at an approximate value of 29 ft when comparing slickwater with the hybrid fluids. Flojet (8gpt) further exhibited the highest value overall. Flojet (8gpt) has friction reducer functioning as a viscosifier in relatively large amount and thus, has an inherent high viscosity. This increased viscosity enables the fluid to overcome stress barriers.

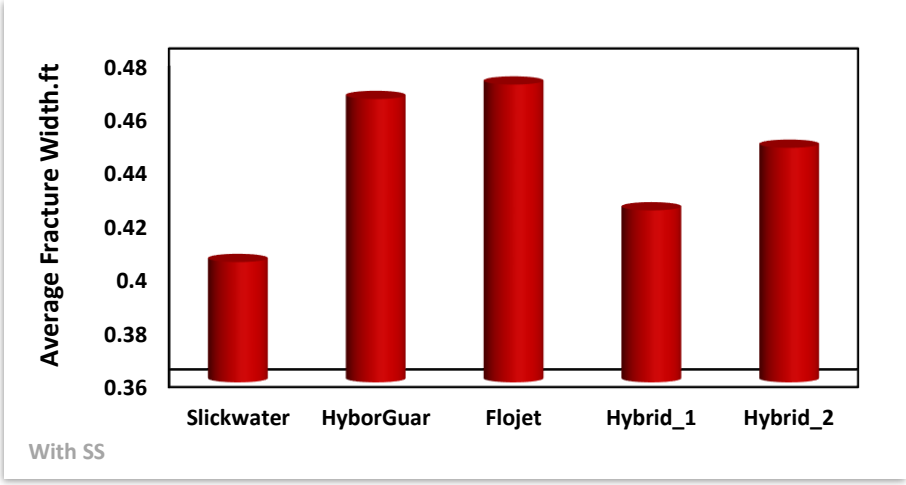

Figure 4.4 Average Fracture Width for all fluid types with stress shadow effect

The shear thinning ability of fluids increases with the amount of polymer in the fluids. This shear thinning ability enables fluids to pass through the relatively small-sized perforations at high shear rates. Upon fracture creation after passage through the perforation, the viscosity of the fluids tend to increase (low shear rates). At this point, fluids' ability to suspend proppants in the fracture and also experience low leak-off rates, largely through viscosity, increases the fracture width. Slickwater, due to its low polymer content and high water content (Newtonian fluid), exhibit a relatively low proppant carrying ability and high leak-off. Flojet (8gpt) and Hybor Guar gave the highest average fracture widths with an approximate difference of 0.005 ft.

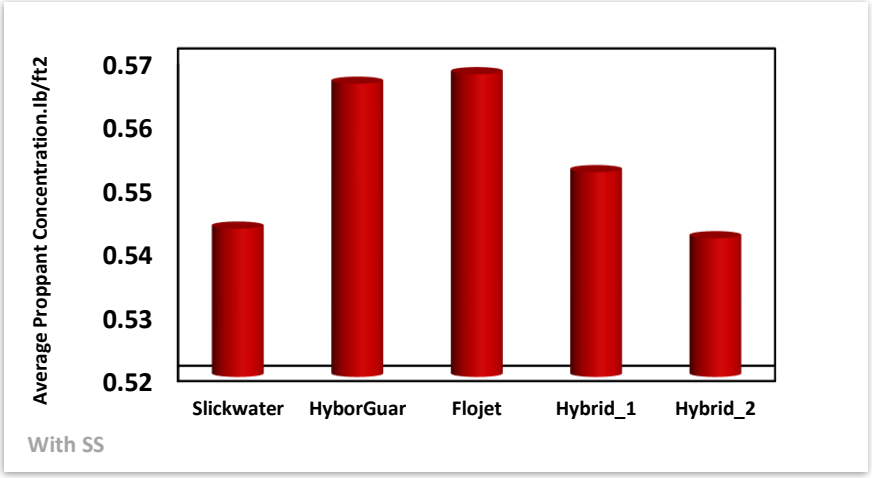

Figure 4.5 Average Proppant Concentration for all fluid types with stress shadow effect

Among slickwater and the hybrid fluids, Hybrid_1 gave the highest average proppant concentration. This was however, inferior to that exhibited by Flojet (8gpt) and Hybor Guar. When the fracture heights of all fluids align with the desired formation (payzone), the proppants suspended by these fluids remain confined within the fracture. This is what happened. As a result, viscous fluids exhibit higher proppant concentration, thanks to their superior proppant suspension (carriage) and more effective distribution.

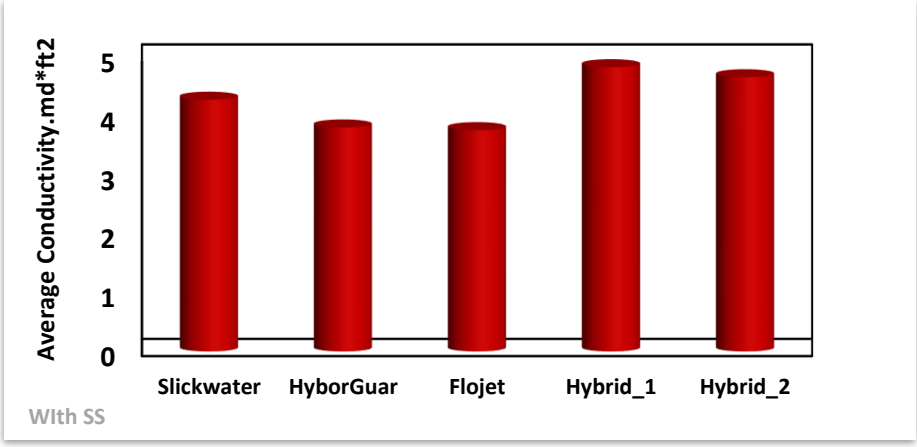

Figure 4.6. Average Fracture Conductivity for all fluid types with stress shadow effect

Hybrid_1 and Hybrid_2 portrayed higher average conductivities as compared to the other fluids. Fracture Conductivity encompasses the ability of fractures to sustain efficient hydrocarbon flow. This is enhanced primarily by the proppant being able to keep fracture open after pumping. Highly viscous fluids enable proppant suspension during pumping, however, after pumping, their low leak-off due to the long fracture closure time resulting from their creation of wider fractures, will favor proppant settling. Whiles proppant settle, the top portion of the fracture easily succumbs to closure stress. Closure of the top fracture part subsequently reduces the contact area. This then negatively affect conductivity. It is therefore desirable to have less viscous fluid in the fracture after pumping in order to keep fractures open (as this has high leak off). In light of this, hybrid fluids, are more likely to give high fracture conductivities. In addition to this, 100 % Flojet (8gpt)

and Hybor guar are more at risk of their polymers getting plugged in the fractures after treatment, thus reducing efficient flow of hydrocarbons.

4.2.1.2. Estimated Fracture Properties without Stress Shadow Effect

Fracture properties under no stress shadow interference generally proved higher in value than those estimated under stress shadow. Table 3 below show the values of the various fracture properties for all fluids used in this study. Also, figures 4.7 – 4.11 are graphical representations of the estimated average fracture properties associated with each fluid without the effect of stress shadow.

Table 3. Average Fracture Properties (with no stress shadow interference)

Average	Slickwater	Hybrid_1	Hybrid_2	HyborGuar	Flojet
Avg. Fracture Half Length.ft	376.4661654	335.7744361	340.9172932	322.8721805	350.7067669
Avg. Fracture Height.ft	25.25166155	29.05123667	27.73608855	34.71847	37.33698767
Avg. Conductivity.md*ft2	8.321110263	8.975338571	8.444463534	9.721714628	8.215464579
Avg. Proppant Conc. Ib/ft2	0.950199342	0.911446207	0.91817447	0.96130047	0.93253368
Avg. Fracture width.ft	0.717389083	0.710663402	0.720847352	0.803674073	0.792473328

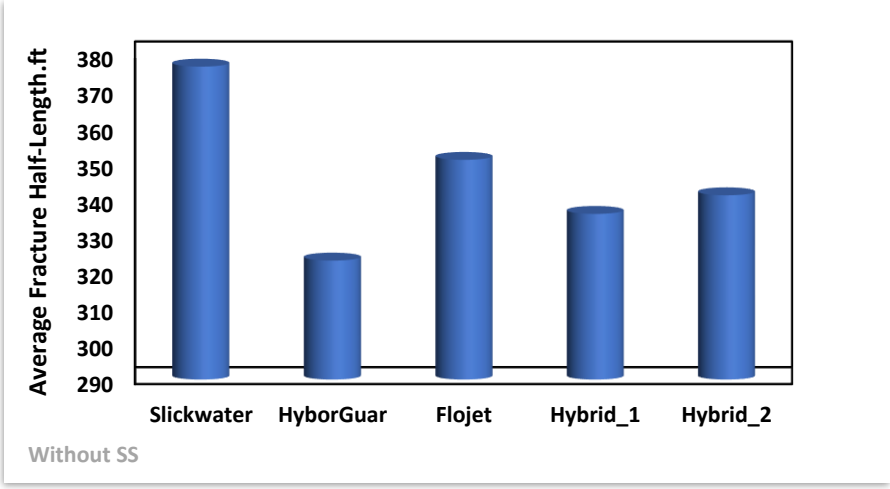

Figure 4.7. Average Fracture Half-Length for all fluid types without stress shadow effect

Slickwater gave the highest value, followed by Flojet (8gpt) with an average difference of 26 ft.

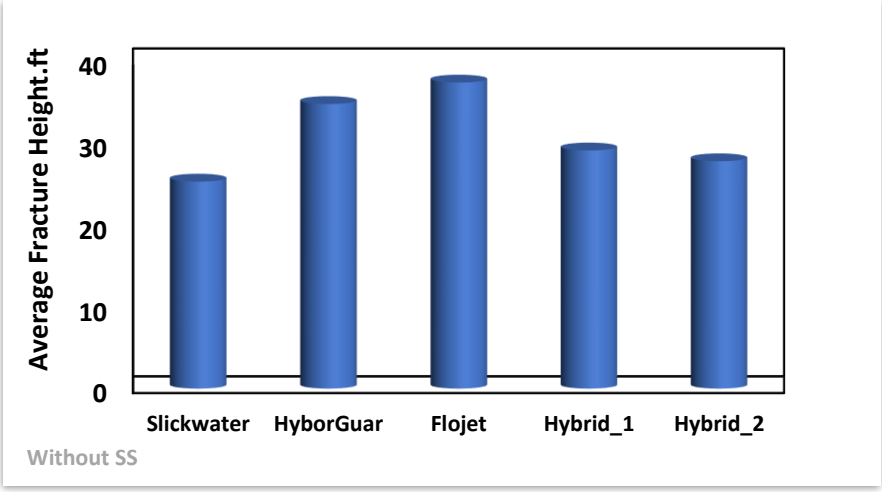

Figure 4.8. Average Fracture Height for all fluid types without stress shadow effect

Hybrid fluids gave high average fracture heights but these were inferior to those produced by the full percentage Flojet (8gpt) and Hybor Guar fluids.

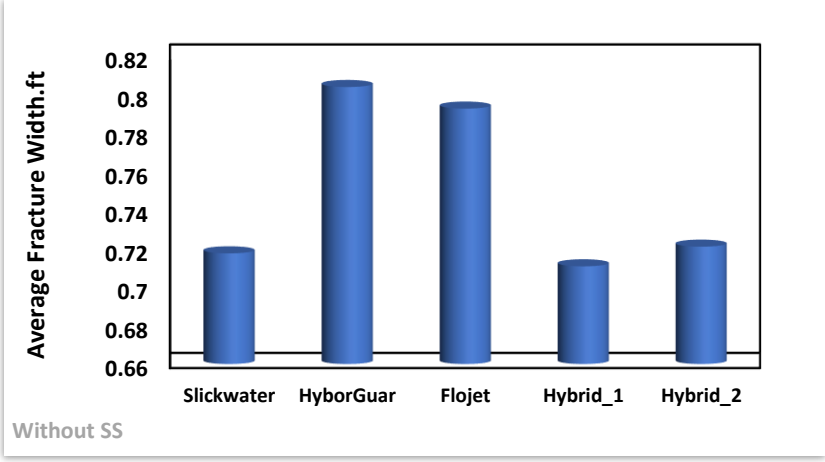

Figure 4.9. Average Fracture Width for all fluid types without stress shadow effect

Hybor Guar exhibited the highest average fracture width when stress shadow was not considered and was followed by Flojet (8gpt).

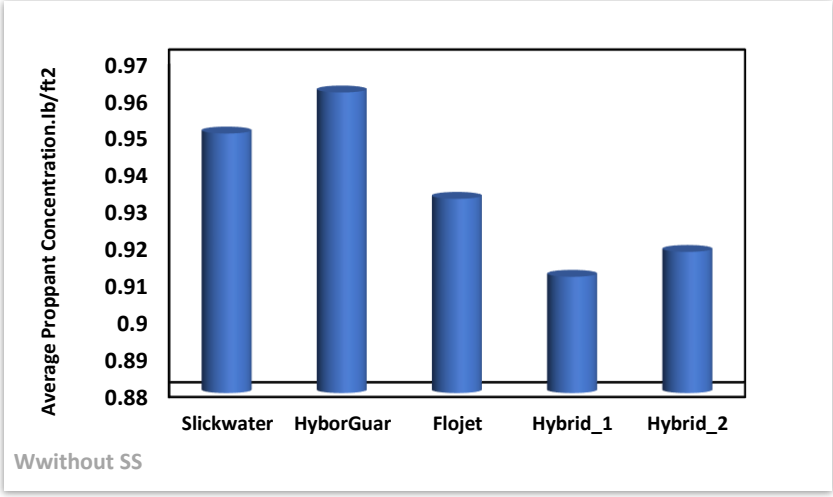

Figure 4.10. Average Proppant Concentration for all fluid types without stress shadow effect

The average proppant concentration was seen to be highest with slickwater when compared with hybrid fluids; a difference of 0.039 between its value and that of the least (hybrid_1). However, among the 100% fluids, HyborGuar portrayed a higher proppant concentration than slickwater (a difference of 0.0111) and also gave the overall highest. Between HyborGuar and Flojet (8gpt), the difference in proppant concentration was 0.029.

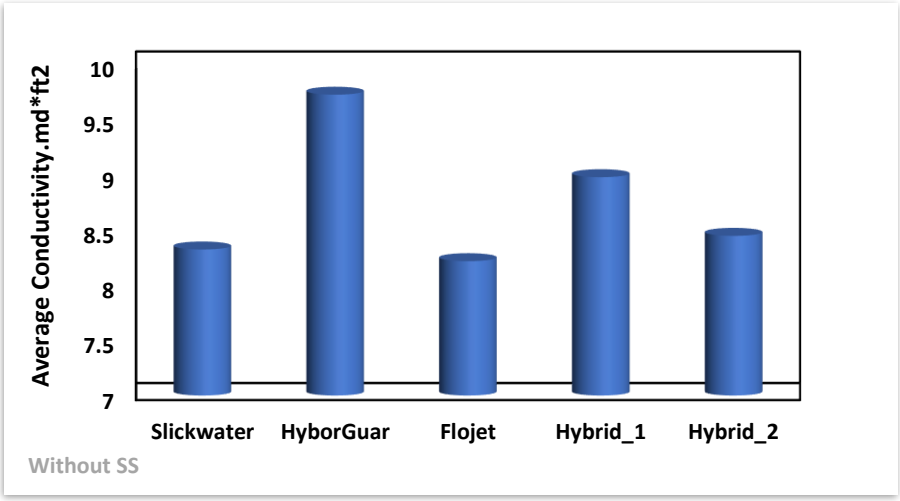

Figure 4.11. Average Fracture Conductivity for all fluid types without stress shadow effect

Hybrid_1 gave the highest average fracture conductivity among slickwater and the hybrid fluids. This is however inferior to that exhibited by the full Hybor Guar fluid in the second set of percentage.

4.2.1.3. Fracture Volume

The fracture volume which encompasses the actual physical space occupied by the hydraulic fracture within the rock formation was determined from the parameters: fracture height, fracture width, and fracture length. Equation 17 below was used for this calculation.

$$FV = ((2x_f * h * (\frac{w}{12}))_{cluster1} + ((2x_f * h * (\frac{w}{12}))_{cluster2} + \cdots + ((2x_f * h * (\frac{w}{12}))_{cluster256} \quad (17)$$

where: x_f is fracture half-length in inches; h is fracture height in inches; and w is fracture width in feet.

The following table (4) displays the overall fracture volumes determined for each fluid.

Table 4. Average Fracture Volume resulting from the usage of each fluid

	Slickwater	HyborGuar	Flojet (8gpt)	Hybrid_1	Hybrid_2
With SS	173,823.98	315204.9701	344842.9607	197436.2838	187589.9459
Without SS	310,412.89	421108.085	496757.2668	320425.7709	312778.8469

4.2.1.3.1. Estimated Fracture Volume under Stress Shadow Effect

Figure 4.12 below graphically show the fracture volumes for all fluid types with stress shadow interference.

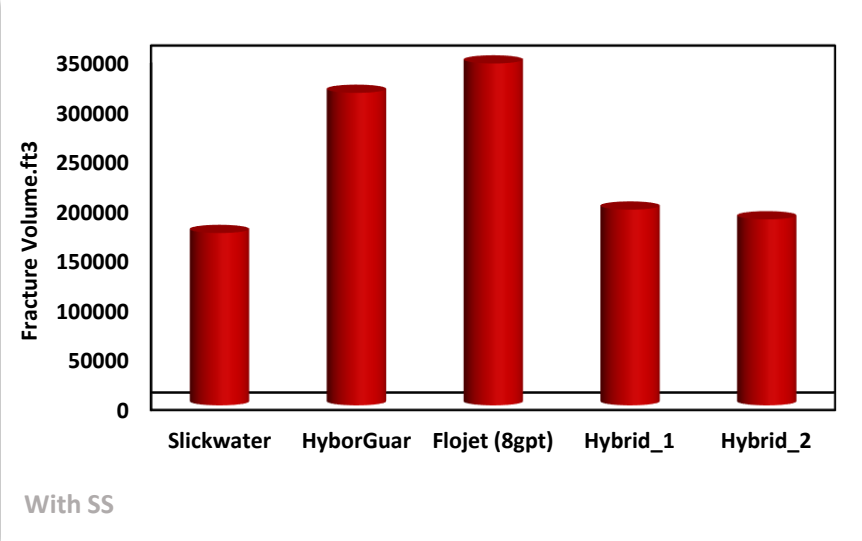

Figure 4.12. Average Fracture Volume for all fluid types with stress shadow effect

Hybrid_1 produced the highest average fracture volume when making a comparison between slickwater and hybrid fluids whereas the solely viscous fluids gave the highest average fracture volume among the 100% fluids. This is attributed to the high fracture height and fracture widths exhibited by them. Flojet (8gpt) gave the highest fracture volume in totality.

4.2.1.3.2. Estimated Fracture Volume without Stress Shadow Effect

Figure 4.13 below graphically show the fracture volumes for all fluid types without stress shadow interference.

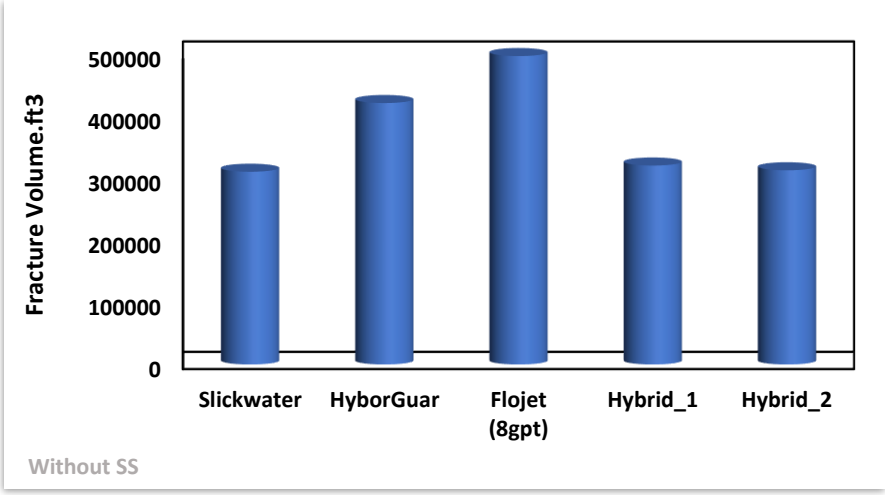

Figure 4.13. Average Fracture Volume for all fluid types without stress shadow effect

Similar to scenario 1, hybrd_1 produced the largest fracture volume in among the hybrid fluids while Flojet (8gpt) gave the overall highest value.

4.2.1.3.3. Impact of Stress Shadow on Fracture Volume

The following chart (figure 4.14) displays a qualitative impact of stress shadow on the fracture volume. The wide gap between values under stress shadow effect and their corresponding values without stress shadow effects indicate the adverse impact of stress shadow in fracture volume (geometry).

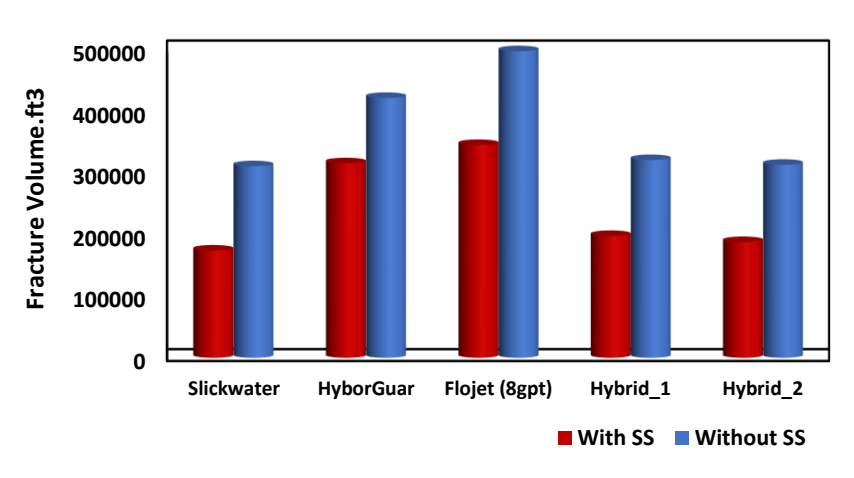

Figure 4.14. Stress Shadow effect on Fracture Volume for all fluid types

4.2.2. Production

Cumulative gas recovery was predicted using each of the fluids and the production values after 1 year, 5 years, 10 years, 15 years and 20 years were recorded. Table 5 below indicates the various cumulative production values predicted under stress shadow effect for each fluid in MMSCF. Also, figures 4.15 – 4.19 are graphical representations of the predicted production performance of each fluid after 1 year, 5 years, 10 years, 15 years and 20 years respectively.

4.2.2.1. Predicted Cumulative Gas Recovery under Stress Shadow Effect

Table 5. Cumulative Gas Recovery (MMSCF)

	Slickwater	Flojet (8gpt)	HyborGuar	Hybrid_1	Hybrid_2
After 1yr	4118.737305	4795.401367	4647.650391	4475.200195	4322.145996
After 5yrs	7386.900879	8147.876953	7947.050293	7780.074219	7596.187012

After 10yrs	9822.182617	10571.70215	10346.95996	10195.7041	10010.61035
After 15yrs	11556.88672	12280.66016	12045.13477	11906.98438	11726.56348
After 20yrs	12931.73438	13631.25488	13389.94727	13263.625	13088.02246

Hybrid fluids performed better than slickwater but they were outperformed by the their solely viscous components. For a period of 20 years, Flojet (8gpt) was observed to produce the highest cumulative gas with Slickwater giving the least production.

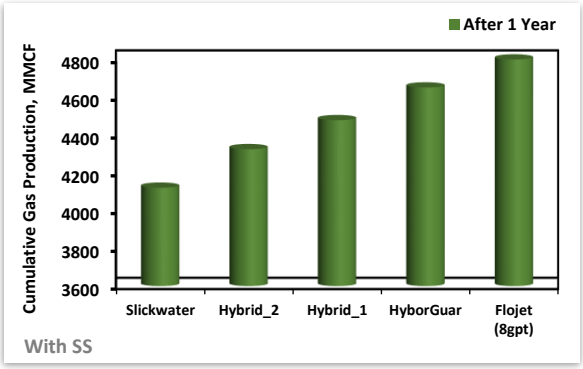

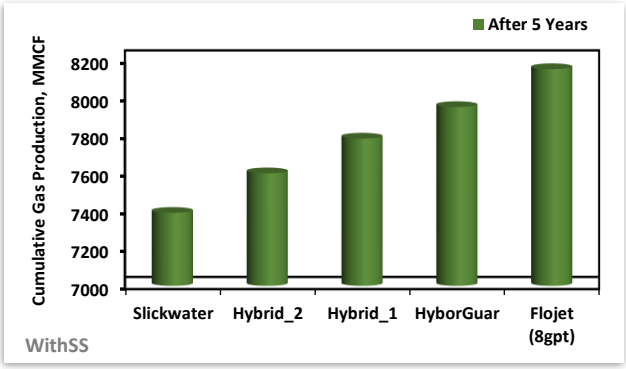

Figure 4.15. Cumulative Production for all fluid types after 1 Year *Figure 4.16. Cumulative Production for all fluid types after 5 Years*

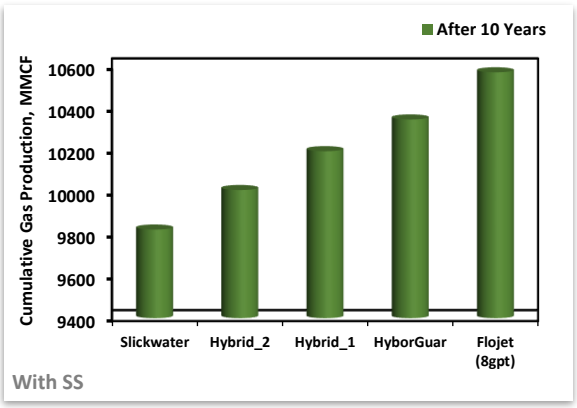

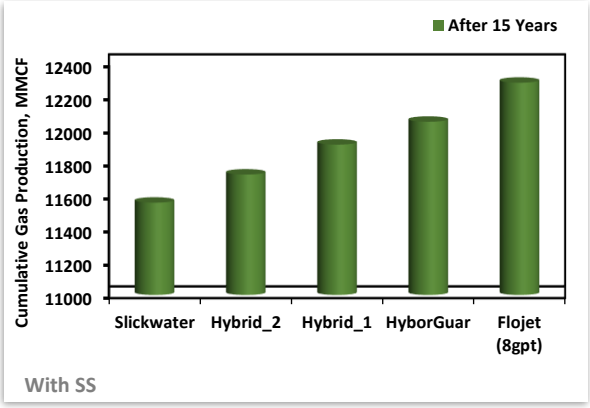

Figure 4.17. Cumulative Production for all fluid types after 10 Years. *Figure 4.18. Cumulative Production for all fluid types after 15 Years*

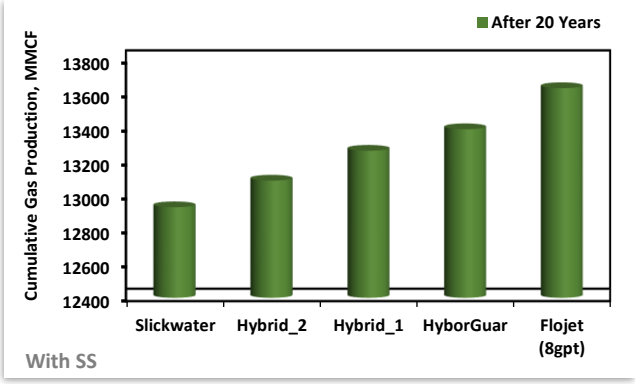

Figure 4.19. Cumulative Production for all fluid types after 20 Years

4.2.2.2. Production Increase Relative To Slickwater

Given the widespread use of Slickwater in the industry, primarily because of its cost-effectiveness, it became essential to quantitatively evaluate the production enhancement achieved by alternative fluids compared to Slickwater. This was determined using equation 18. Table 6 shows the increase in production relative to slickwater, expressed as percentages, while figure 39 illustrates their graphical representations.

$$Percent \text{ Increase} = \frac{Production\ value\ of\ fluid_i - Production\ value_{\ Slickwater}}{Production\ value_{\ Slickwater}} \quad (18)$$

Where i is the fluid under consideration (except slickwater)

4.2.2.2.1. Production Increase Relative To Slickwater under Stress Shadow Effect

From Figure 4.20, cumulative gas recovery obtained using Flojet (8gpt) was approximately 16% higher than that produced from Slickwater after the first year. This is a significant increase and as such, justifies the decision to opt for a relatively costly High Viscosity Friction Reducer (Flojet_8gpt) for this Marcellus Shale horizontal well, as the cost increase can be offset by the production enhancement, all things being equal.

Table 6. Percent Increase in Production relative to Slickwater

	% Inc. Flojet (8gpt)	% Inc. HyborGuar	% Inc. Hybrid_1	%Inc. Hybrid_2
After 1 yr	16.42892014	12.84163196	8.654664384	4.938617745
After 5yrs	10.30169602	7.583009753	5.322575006	2.833206188
After 10yrs	7.630885721	5.342777306	3.80283588	1.918389651

After 15yrs	6.262702531	4.224736807	3.029342283	1.468187429
After 20yrs	5.409332482	3.543321241	2.566481922	1.208562452

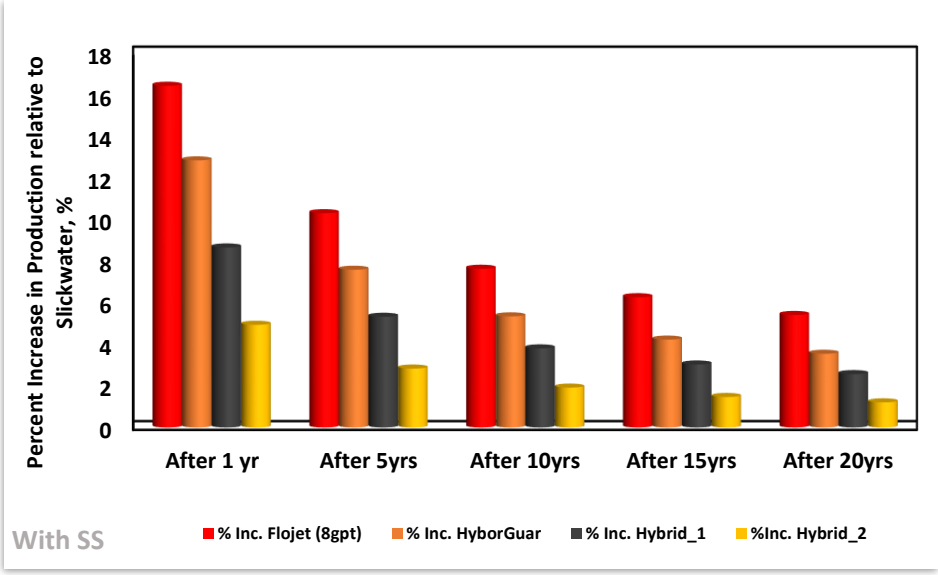

Figure 4.20. Percent Increase in Production as compared to Slickwater with Stress Shadow effect

4.2.2.3. Effect of Stress Shadow in Production

The impact of stress shadow in production was also assessed, with results shown in table 7. Decrease in production (expressed as percentages) resulting from that was calculated by equation 19 below. Figure 4.21 depicts a graphical illustration of the impact of stress shadow in production for all fluid types.

It can be seen that all fluids were impacted by stress shadow percentages with little differences among them. The highest stress shadow impact of approximately 23% after one year indicates the adverse effects of this occurrence. Nevertheless, this impact declines with time.

$$Percent\ Reduction\ of\ \text{Prod.} = \frac{Production\ value\ of\ fluid_{without\ SS} - Production\ value\ of\ fluid_{withSS}}{Production\ value\ of\ fluid_{withoutSS}} \qquad (19)$$

Table 7. Percent Decrease in Production, %

	Slickwater	Flojet (8gpt)	HyborGuar	Hybrid_1	Hybrid_2
After 1 yr	20.04682	20.34974159	22.6132028	18.49504	17.6674292
After 5yrs	17.287317	18.69515456	19.71182	15.92665	15.1058566

After 10yrs	15.566183	17.62161865	18.0050151	14.37513	13.5308718
After 15yrs	14.488624	16.92219472	16.9637714	13.4364	12.5689481
After 20yrs	13.734797	16.3793576	16.1967408	12.76042	11.8847081

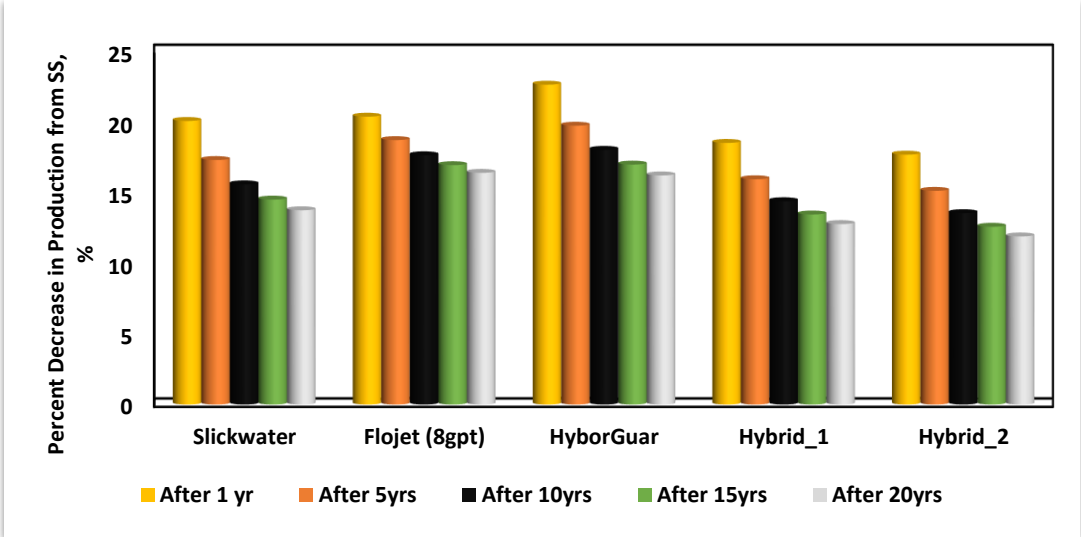

Figure 4.21 Impact of Stress Shadow in Production for all Fluid Types

CHAPTER 5: CONCLUSIONS

Conclusion

In this study, the effect of fracturing fluids on hydraulic fractures and gas production from a Marcellus shale horizontal well was studied. Fluids used for the study are Slickwater, 100% Flojet (8gpt) which is a High Viscosity Friction Reducer (HVFR), 100% Hybor Guar which is a Crosslinked Gel, a hybrid fluid of Slickwater and Flojet (8gpt), and a hybrid fluid of Slickwater and Hybor Guar. The following observations were made:

- The utilization of slickwater as a fracturing fluid resulted in the formation of hydraulic fractures in only the lower Marcellus shale, as it couldn't overcome the stress barriers between the lower and upper Marcellus shale layers. The High Viscosity Friction Reducer (HVFR) and Hybor Guar (XL gel), however, effectively surmounted these stress barriers between, facilitating the occurrence of elevated fracture levels in the upper Marcellus shale (increased fracture heights).

- Though slickwater was able to create long fractures, it gave low fracture heights due to its less ability to overcome stress barrier. This characteristic is as a result of its low viscosity.

- Hybrid fluids were found to have the highest conductivity. This is due to their ability to prevent proppant settling after pumping as compared to 100% Flojet and 100% Hybor Guar. The wider fractures created by these 100% different fluids increases the closure time thus favoring proppant settling after pumping.

- The HVFR (Flojet_8gpt) caused the greatest fracture volume, fracture height, increase in production, as well as the highest overall production, when compared to the different fluids used in this study and also slickwater. It is recommended to use HVFR (Flojet_8gpt) for Marcellus Shale horizontal wells.

- After one-year, different fracturing fluids yield significant improvements in cumulative gas recovery compared to slickwater. However, as time passes, it will decrease.

- HVFR's (Flojet_8gpt) significant increase in production relative to slickwater makes present some justification to its usage in the Marcellus Shale horizontal well, against its costliness.

- All fluid types were significantly impacted by stress shadow.

- To accurately predict the hydraulic fracture properties in a horizontal Marcellus shale well with multiple hydraulic fracture stages, the impact of the stress shadowing must be considered.

- The adverse impact of the stress shadowing on production is more pronounced during early production due to higher production rates.

References

1. Alexander C. Barbati, Jean Desroches, Agathe Robisson, and Gareth H. McKinley. Complex Fluids and Hydraulic Fracturing. 2016.
2. Alotaibi, N.; Dursun, S.; Optimizing the Hydraulic Fracturing Fluid Systems Using the Completion and Production Data in Bakken Shale. Presented at the Middle East Oil, Gas and Geosciences Show held in Manama, Bahrain, 19 – 21 February 2023. SPE-213360-MS
3. Barati, R.; Liang, J. A Review of Fracturing Fluid Systems Used for Hydraulic Fracturing of Oil and Gas Wells. Journal of Applied Polymer Science, 2014.
4. Faraj A. Ahmad, Jennifer L. Miskimins. An Experimental Investigation of Proppant Transport in High Loading Friction-Reduced Systems Utilizing a Horizontal Wellbore Apparatus. URTEC. July 2019.
5. Feng Li et. al (2016) A comprehensive review on proppant technologies.
6. Gadde, P., Yajun, L., Jay, N., Roger, B., Sharma, M., 2004. Modeling proppant settling in water-fracs. In: Proc. SPE-89875-MS, SPE Annu. Tech. Conf. Exhib, September 2629, Houston, TX.
7. Hoss B., Ebrahim F., Fatemeh B., Hydraulic Fracturing in Unconventional Reservoirs. Theories, Operations, and Economic Analysis. Elsevier, 2017.
8. J. Bellarby, Well completion design, Amsterdam: Elsevier B.V., 2009.
9. Kitchen, J.; Kakadjian, S.; Vu, J.; Hundt, N. Successfully Optimizing Performance of Friction-Reducer Boosters for Slickwater and High-Viscosity Fluids. Presented at the SPE International Conference on Oilfield Chemistry held in The Woodlands, Texas, USA, 28 – 29 June, 2023. SPE-213803-MS
10. Kolawole, O.; Ispas, I. Interaction between hydraulic fractures and natural fractures: current status and prospective directions. Journal of Petroleum Exploration and Production Technology. Published in 2019
11. Kolawole, O.; Marshal, W.; Ion, I.; Marshall, W. How will treatment parameters impact the optimization of hydraulic fracturing process in unconventional reservoirs? Springer Nature. Published October 2020.

12. Koray, A.; Bui, D.; Ampomah, W.; Appiah-Kubi, E.; Klumpenhower, J. Improving Subsurface Characterization Utilizing Machine Learning Techniques. Paper presented at the SPE Western Regional Meeting held in Anchorage, Alaska, USA, 22 - 25 May 2023. SPE-212952-MS
13. Koray, A.; Bui, D.; Ampomah, W.; Appiah-Kubi, E.; Klumpenhower, J. Application of Machine Learning Optimization Workflow to Improve Oil Recovery. Paper presented at the SPE Oklahoma City Oil and Gas Symposium, held in Oklahoma City, Oklahoma, USA, 17-19 April 2023. SPE-213095-MS.
14. Neal B. Nagel. Hydraulic Fracturing in Unconventionals: The Necessity of a New Geomechanics Paradigm. Geomechanics for Unconventionals Series, Vol XIII.
15. Pater, C.; Prabhakaran, R.; Shaoul, J. Observations and Modeling of the Relation Between Effective Reservoir Stress and Hydraulic Fracture Propagation Pressure. Presented at the SPE Hydraulic Fracturing Technology Conference and Exhibition held in The Woodlands, Texas, USA, 24-26 January 2017. SPE-184831-MS
16. Rozhko, A. Capillary Phenomena in Partially-Saturated Rocks: Theory of Effective Stress. Presented at the 45th US Rock Mechanics / Geomechanics Symposium held in San Francisco, CA, USA. in 2011. ARMA 11-146
17. R.D. Barree. Modeling Fracture Geometry. Barree & Associates LLC
18. Sgher, M.; Aminian, K.; Matey-Korley, V.; Ameri, S. Impact of Stress Shadow on the Proppant Transport and the Productivity of the Multi-Staged Fractured Marcellus Shale Horizontal Wells. Presented at the 57th US Rock Mechanics/Geomechanics Symposium, Atlanta, Georgia, USA, June 2023. ARMA 23– 0811
19. West Virginia Research Corporation. Final Scientific/Technical Report of the Marcellus Shale Energy and Environment Laboratory (MSEEL). Prepared for United States Department of Energy; National Energy Technology Laboratory. Report issued in December 2021.
20. Yongpeng Sun, SPE; Hao Zhang, SPE; Qihua Wu; Mingzhen Wei, SPE; Baojun Bai, SPE; Yinfa Ma. Experimental Study of Friction Reducer Flows in Microfracture During Slickwater Fracturing. SPE 164053. 2013.